The temperature coefficient of a PWR based on an in-rod heterogeneous thorium/uranium fuel design

A Blennies

orcid.org/0000-0002-2155-8738

Mini-Dissertation accepted in partial fulfilment of the requirements for the degree *Master of Sciences in Engineering Sciences with Nuclear Engineering* at the

North-West University

Supervisor:	Prof F van Niekerk
Co-Supervisor:	Mr HB van der Walt

Graduation:	May-June 2023
Student number:	30106052

ABSTRACT

The effect of temperature change in nuclear reactors is of high importance due to the influence on the reactivity of the reactor and its implication for reactor safety. The temperature coefficient of reactivity due to change of either fuel or moderator temperature determines the temperature and hence reactivity feedback properties of the fuel; the reactor and fuel have to be designed to be safe under normal operating conditions as well as postulated transients following initiating events. In this study, the change of reactivity as a function of the temperature of fuel and moderator is investigated for thorium-uranium equilibrium fuel designs proposed by Van der Walt (2015) and compared to reference equilibrium fuel. In addition, the delayed neutron fraction is determined for these fuel models to determine the impact on the safety and control of the reactor.

The study aims to simulate the effect of temperature change in the moderator and fuel using the MNCP 6.2 code to model the fuel pin reactivity at the beginning of cycle (BOC), middle of cycle (MOC) and end of cycle (EOC), and SERPENT 2.1 on the full-core reactivity at BOC respectively on the proposed fuel models. Furthermore, the influence of boron on the Moderator Temperature Coefficient (MTC) will be investigated when the density of the coolant changes with the change of temperature at constant boron concentration. A delayed neutron fraction will be calculated due to its influence on the safety and control of the proposed fuel designs and reference fuel.

Using the calculated k_{eff} values at different temperatures (simulated with MCNP 6.2), reactivity and k_{eff} as a function of temperature (for both the fuel and the coolant) are obtained for the proposed fuel designs and reference fuel. A function with a form based on the underlying physics is fitted to the simulated data points in a procedure which rendered the optimal equation constants. By differentiating the equations, the Fuel Temperature Coefficient (FTC) and Moderator Temperature Coefficient (MTC) were derived. Delayed neutron fraction is calculated using the prompt method, where the first criticality calculation using MCNP (Monte Carlo Neutron-Particle) is performed to find the prompt effective multiplication factor k_p (which includes only prompt neutrons) and lastly followed by a second criticality calculation to find the total effective multiplication factor (which includes prompt and delayed neutrons). At BOC, the

effective multiplication factor curves for the fuel temperature change show that an increase in the temperature of the fuel will result in a decrease in k_{eff} for all the fuel designs (including reference fuel). Due to the negative slope of the curves between k_{eff} and fuel temperature, the FTC is negative for all the fuel models. All Moderator Temperature Coefficients calculated at 0ppm and 1000ppm conditions are negative except for the 5Th1U (5cm Th and 1cm U axial loaded) fuel design when 1000ppm boron is present. All the k_{eff} curves as a function of moderator temperature have a negative slope, except the 5Th1U fuel design. A reduction in coolant density due to an increase in the moderator temperature causes the k_{eff} to decrease. This occurs because of the less neutron moderation that results due to a reduction of the number of coolant atoms present per unit volume of the moderator which is present at BOC, MOC and EOC burnup points. Furthermore, the boron effect is also reduced due to coolant density reduction, because fewer boron atoms are present per unit volume to absorb neutrons, however neutron absorption by the fuel increases which subsequently increases the k_{eff}. At MOC, the FTC is negative for all the fuel designs, however, the reference fuel has a less negative FTC compared to the fuel designs proposed by Van der Walt (2015). The k_{eff} for all the fuel designs is below unity when 1000ppm boron is added. The MTC at 0ppm and 1000ppm conditions is negative for all curves. The EOC for fuel temperature change and moderator temperature change the value of the k_{eff} is above unity and all the curves have a negative gradient. Therefore, FTC and MTC are negative at all temperature points at EOC.

The k_{eff} curves for a full-core as a function of fuel temperature all display a negative slope which is associated with a negative FTC. The increase in fuel temperature results in a decrease in k_{eff} due to Doppler Broadening because fewer neutrons are available for fission thus resulting in a negative FTC. Furthermore, due to equilibrium fuel designs, the fuel matrix also influences neutron absorption. The MTC curves in the absence of boron in the moderator are negative, as mentioned above the MTC is influenced by the reduction in coolant density as the temperature increase which subsequently reduces neutron moderation. In the case of 1000ppm boron in the coolant, the MTC curves are all negative except for the 5Th1U curve due to the reduction in boron effect as the number of boron atoms decrease per unit volume in the moderator.

The delayed neutron fraction decreases as the burnup increases for all the fuel designs except for 5Th1U at MOC with an increase and rapid decrease at EOC. However, due to the depletion of U^{235} in $UO_{2,}$ the β_{eff} decreases and the build-up of U^{233} for thorium-based fuel reduces β_{eff}.

The proposed designs by Van der Walt (2015) for an equilibrium fuel model show that the amount of thorium content influences the reactivity significantly and the change in reactivity due to temperature change. From all the proposed fuel designs by Van der Walt (2015) and the reference fuel, the FTC and MTC of 1Th1U are negative at all burnup points, i.e, BOC, MOC, and EOC. The k_{eff}, MTC and MTC curves for 1Th1U and UO_2 both show slightly similar gradients for all the burnup points. Therefore, the results presented indicate that 1Th1U serves as the best fuel candidate among the proposed fuel designs due to favourable safety characteristics.

Key words: Moderator Temperature Coefficient, Fuel Temperature Coefficient, Reactivity Temperature Coefficient, Delayed Neutron Fraction, Boron Coefficient, Equilibrium Fuel

ACKNOWLEDGEMENTS

Modimo le Badimo ba gaisa bao ba kgatlhanong. Thapelo e falola dikgwetlo tsotlhe tsa botshelo segolobogolo gareng ga moriti wa poifo le loso. Kamogelo e nne tshimologo ya boitumelo le katlo, mme, seo se bake gore botshelo bo tswelele pele, tsotlhe pheletsong ga mmogo le maikutlo dibone kagiso.

I would like to take this moment which will forever exist in writing to thank God and My Ancestors for the protection against all the storms I have faced from the first day of pursuing a master's degree in engineering. The support from my family during all the obstacles which I faced while studying towards this degree I would like to send my greatest appreciation and may all the blessing fall upon you.

Ke rata go leboga mme-motsadi (Gadibolelwe) le bokgaitsadi (Oreeditse, Thebeetsile le Rebaone).

To Prof Frik van Niekerk, my supervisor, this has been a very fruitful and nurturing journey for me, your guidance has absolutely crafted a mark in my personal and academia world which has enhanced my academic skills and above all my personal skills.

To Bernard van der Walt, my co-supervisor, I would like to send my greatest acknowledgements to you with the support and assistance throughout the study.

I dedicate this paper to my daughter Katlo Simvuyele Blennies and my late father Kabelo Aubrey Blennies.

PULA!!!!!!

Table of Contents

1 Introduction 1

1.1 Background 1

1.2 Problem statement 3

1.3 General-purpose of the study 4

1.3.1 Aim 4

1.3.2 Objectives 4

2 Theoretical background 6

2.1 Thorium-based fuel 6

2.2 Effect of delayed neutrons 7

2.3 Temperature effects on reactivity 11

3 Literature review 15

3.1 Heterogeneous thorium fuel designs 15

3.2 Reactivity temperature coefficient 16

3.2.1 Uranium MOX fuel 16

3.2.2 Thorium heterogeneous fuel 17

3.2.3 Effects of neutron poisons 19

4 Methodology 22

4.1 Material and geometry description 23

4.2 Numerical simulations and procedure 24

4.2.1 Use of numerical models 24

4.2.2 Numerical procedure 25

4.3 Method of analysis 26

4.3.1 Deriving the k_{eff} equation and curve-fit approximation function for the FTC and MTC. 28

4.4 Validation calculations: Full-core Serpent model..... 31

5 Results and discussions..... 34

5.1 Fuel pin calculations at BOC, MOC and EOC models 34

5.1.1 Fuel temperature change..... 34

5.1.2 Moderator temperature change. 38

5.1.3 Moderator temperature change with 1000ppm Boron concentration. ... 42

5.1.4 Moderator temperature change with varying boron concentration..... 46

5.1.5 Boron coefficient. 48

5.1.6 Delayed neutron fraction..... 49

5.2 Equilibrium fuel full core calculations at BOC..... 51

5.2.1 Fuel temperature change..... 51

5.2.2 Moderator temperature change without boron..... 52

5.2.3 Moderator temperature change with 1000ppm boron. 54

5.3 Uncertainty in k_{eff} values: MCNP (fuel pin) and SERPENT (full core) results. 55

6 Conclusion and recommendations..... 58

6.1 Conclusions..... 58

6.2 Recommendations 59

References 61

Annexures 64

LIST OF TABLES

Table 1: Data tabulated from MCNP simulation 27

Table 2: Tabulated data of reactivity, k_{eff} and temperature coefficient of reactivity... 28

Table 3: Core loading pattern..... 32

Table 4: H3BO3 concentration and k_{eff} of the fuel models at 550K moderator temperature..... 47

Table 5: Boron coefficients for 550K moderator temperature at BOC 49

Table 6: Delayed neutron fractions at BOC, MOC and EOC..... 50

Table 7: MCNP(fuel pin) and SERPENT(full core) average k_{eff} (fuel) value comparison at BOC 56

Table 8: Error bounds of the MCNP code calculated k_{eff} at MOC..... 57

LIST OF FIGURES

Figure 1-1: Levelised cost of generating electricity of different energy sources (IEA, 2020) 1

Figure 2-1: Th^{232} and U^{233} fertile-fissile transmutations (Nuclear Energy Agency, 2015) 6

Figure 2-2: Reactor period vs reactivity for a U^{235} fuel (Lamarsh and Baratta, 2002). 9

Figure 2-3: Delay neutron fraction of fissile isotopes (Lamarsh and Baratta, 2002) . 10

Figure 2-4: Doppler-broadening of the absorption resonance of U-238 at 6.67eV (Lamarsh and Baratta, 2002) 13

Figure 2-5: Moderator Temperature Coefficient vs Temperature for different Boron concentration (Oka, 2014) 14

Figure 4-1: Side view of the proposed fuel design model 23

Figure 4-2: Side view of the reference fuel 23

Figure 4-3: Axial view of the proposed fuel design model 24

Figure 4-4: Axial view of a full-core equilibrium fuel design 33

Figure 5-1: k_{eff} vs Fuel temperature at BOC 35

Figure 5-2: k_{eff} vs Fuel temperature at MOC 35

Figure 5-3: k_{eff} vs Fuel temperature at EOC 36

Figure 5-4: FTC vs Fuel temperature at BOC 37

Figure 5-5: FTC vs Fuel temperature at MOC 38

Figure 5-6: FTC vs Fuel temperature at EOC 38

Figure 5-7: k_{eff} vs Moderator temperature without boron at BOC 39

Figure 5-8: k_{eff} vs Moderator temperature without boron at MOC..... 39

Figure 5-9: k_{eff} vs Moderator temperature without boron at EOC 40

Figure 5-10: MTC vs Moderator temperature without boron at BOC..... 41

Figure 5-11: MTC vs Moderator temperature without boron at MOC 41

Figure 5-12: MTC vs Moderator temperature without boron at EOC..... 42

Figure 5-13: k_{eff} vs Moderator temperature with 1000ppm boron at BOC 43

Figure 5-14: k_{eff} vs Moderator temperature with 1000ppm boron at MOC..... 43

Figure 5-15: k_{eff} vs Moderator temperature with 1000ppm boron at EOC 44

Figure 5-16: MTC vs Moderator temperature with 1000ppm boron at BOC 45

Figure 5-17: MTC vs Moderator temperature with 1000ppm boron at MOC 45

Figure 5-18: MTC vs Moderator temperature with 1000ppm boron at EOC 46

Figure 5-19: k_{eff} vs Moderator temperature (varied boron concentration) at BOC 47

Figure 5-20: MTC vs Moderator temperature (varied boron concentration) BOC..... 48

Figure 5-21: k_{eff} vs Fuel temperature of a full core at BOC..... 51

Figure 5-22: FTC vs Fuel temperature of a full core at BOC..... 52

Figure 5-23: k_{eff} vs Moderator temperature of a full core without boron at BOC 53

Figure 5-24: MTC vs Moderator temperature of a full core without boron at BOC ... 53

Figure 5-25: k_{eff} vs Moderator temperature of a full core with boron at BOC..... 54

Figure 5-26: MTC vs Moderator temperature of a full core with boron at BOC 55

Figure 0-1: Cell card for 300K Input file..... 64

Figure 0-2: Material card 300K input file..... 64

Figure 0-3: Cell card for 550K Input file..... 64

Figure 0-4: Material card 550K input file..... 65

LIST OF ABBREVIATIONS AND SYMBOLS

U^{233}	Uranium 233
U^{235}	Uranium 235
U^{238}	Uranium 238
Th^{232}	Thorium 232
Pa^{233}	Protactinium 233
Pu^{239}	Plutonium 239
UO_2	Uranium Oxide
ThO_2	Thorium Oxide
Th-U	Thorium-Uranium
Gd_2O_3	Gadolinia
U-B1	Uranium-Boron
3Th1U	3cm Thorium-1cm Uranium
η-value	Eta
k_{eff}	Effective Multiplication Factor
L_p	Prompt neutron lifetime
k_∞	Infinite Multiplication factor

β_{eff}	Effective delayed neutron fraction
$\emptyset_T$	Neutron flux
p	Resonance escape probability
α_T	Temperature Coefficient of Reactivity
ρ	Reactivity
I	Resonance integral
MCNP	Monte Carlo N-Particle
BOC	Beginning of Cycle
MOC	Middle of Cycle
EOC	End of Cycle
MTC	Moderator Temperature Coefficient
FTC	Fuel Temperature Coefficient
MOX	Mixed oxide
LCOE	Levelised Cost of generating Electricity
LEU	Low Enriched Uranium
HEU	High Enriched Uranium
KCODE	Criticality Calculation Code

ThN	thorium mononitride
UN	Uranium mononitride
IFBA	Integral fuel burnable absorber
Standard Deviation	St Dv
PCM/pcm	Per cent mille

1 Introduction

1.1 Background

Research and development of thorium as a fertile element in the nuclear industry is motivated i.e. by the cost and availability of uranium. An increase in energy demand is influenced by the global economic and population growth. Nuclear energy is regarded as a clean energy source: energy production is not based on fossil fuel, and all radioactive waste is captured and safely disposed. The externality cost of nuclear energy is typically diligently calculated and presented in energy trade-off or comparison studies. While both nuclear and renewable energy are regarded as clean energy, nuclear energy is also considered ideal for baseload energy generation – due to the intermittent nature of renewable energy, energy storage needs to be supplied in addition to the supply of renewable energy. Furthermore, the expected levelised cost of generating electricity (LCOE) from nuclear power is relatively low in comparison to other energy sources, despite the capital cost of constructing a nuclear power plant being high. Figure 1-1 shows both newly built and lifecycle extended nuclear power plants have low LCOE in comparison to fossil fuel and low carbon energy generation technologies (International Energy AgencyIEA, 2020).

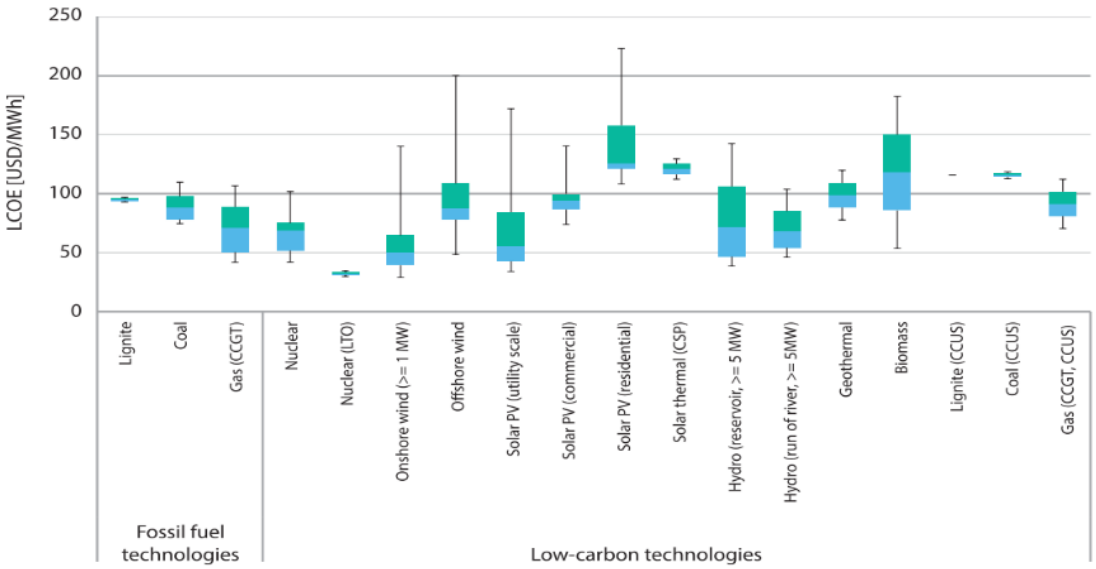

Figure 1-1: Levelised cost of generating electricity of different energy sources (IEA, 2020)

Reactor safety is a fundamental prerequisite in nuclear reactor design – no compromise is allowed in safety when seeking a trade-off between various reactor design parameters. In fulfilling the primary objective of a reactor to produce power, any negative impact on the environment and living organisms should be avoided at all costs. Hence appropriate design and construction of the facility, extensive process authorization control and the necessary quality standards have to be in place in design, construction, and operation. The essential attributes to ensure the safety of nuclear reactors are to contain radioactive inventory during normal operation and any postulated design base accident scenario. Inherently safe reactors achieve this goal by relying on designs which utilise inherent safety characteristics and rely on passive safety mechanisms. Conventional reactors (e.g. PWRs) rely on optimised design and safety systems to ensure the containment of radioactive inventory. These safety systems employ the principles of defence-in-depth (e.g. by virtue of design principles such as redundancy and diversity) to ensure system integrity and to keep exposure to radioactivity as low as reasonably achievable (ALARA). Conditions which will cause a breach in material integrity (e.g. exposure to heat, excessive fluence or mechanical load) outside design limits are to be avoided in all circumstances. Given the high power density of PWRs, the safe removal of heat has to be achieved without compromise. In addition, any operational condition which may lead to an undue increase in heat generation has to be avoided. In this regard operability and control of the reactor are safety requirements, which necessitates due consideration to be given to temperature coefficient and delayed neutron fraction.

The effective multiplication factor (k_{eff}) is the ratio of the number of neutrons available for staring the next life-cycle in one generation divided by the number of neutrons lost through absorption in the previous generation. For a constant power operation of the reactor, the neutron production rate and neutron loss rate should remain equal respectively, resulting in an effective multiplication factor (k_{eff}) equal to one. Factors influencing the neutron multiplication include, among others, reactor layout and materials, fissile inventory, moderation, and neutron absorbers (burnable absorbers, control rods and other core materials). Operational conditions such as operating temperature also influence the neutron population and hence reactivity. The Temperature Coefficient of Reactivity α_T indicates the influence of a change in

temperature on reactivity. In this study the change of reactivity as a function of the temperature of fuel and moderator of a thorium-containing fuel design proposed by Van der Walt (2015) will be investigated, i.e. the fuel temperature coefficient (FTC) and moderator temperature coefficient (MTC) will be determined. The FTC is a function of the fuel composition and reactor design, and it is required that the FTC to be negative to ensure a controllable reactor. Furthermore, the importance of a negative MTC plays a role in ensuring that the amount of energy extracted from the turbine is proportional to the amount of heat removed or generated by the reactor that is when more power is required by the turbine, heat generation from the pressurised water reactor increase, thus an increase in temperature. In case of an opposite event, the temperature drops to ensure that the reactor doesn't heat up leading to any possible physical damage to the fuel (Lamarsh and Baratta, 2002).

A negative reactivity feedback mechanism has a direct and significant influence on the safe operation of a nuclear reactor. Therefore, a reactor needs to be designed such that any change in power from the turbine due to load demand, the temperature of the reactor is required to change to prevent any possible incident or power failure (through reactor shutdown). This study focuses on the safety implications of the temperature coefficient of a set of fuel designs incorporating thorium in a PWR, proposed by Van der Walt (2015).

1.2 Problem statement

In order to introduce thorium-based fuel as an alternative fuel in nuclear reactors, a range of fuel design criteria have to be met, which include criteria related to safety and neutron economy. Van der Walt (2015) proposed axial heterogeneous thorium-based fuel designs which achieved high fuel burnup, primarily due to the build-up of U^{233}, which has a greater η-value (ratio of neutrons produced per neutrons absorbed in the fuel for each fission reaction) than U^{235}. Besides the enhanced economic benefits, it has to be shown that all safety criteria of the reactor by the use of this proposed fuel are met. Several researchers, working on thorium-based fuel, have reported limitations concerning the temperature coefficients of such fuel, such as Tucker, Alajo and Usman (2015), du Toit and Naicker (2018) and Humphrey, Sani and Uddin (2020) among others. Therefore, safety analysis of the effect of temperature variation in both fuel and

moderator is essential including thorium-based heterogeneous fuel. Furthermore, when introducing new fuel to a reactor, it is important to determine the value of the delayed neutrons which are important for the control of a reactor. Since thorium-containing fuel will lead to a different material matrix to burn as in the case of conventional fuel (it should be expected that the fraction of delayed neutrons will change over time since the burnup, in this case, will not only include U^{235}, Pu^{241} and Pu^{239} isotopes, but also the build-up and burnup of U^{233}). Since the different elements have different decay fission products with different neutron decay characteristics, it should be expected that β_{eff} for various proposed fuel models will differ, hence it is important when to determine β_{eff} when introducing any conventional fuel concept.

1.3 General-purpose of the study

1.3.1 Aim

The purpose is to ascertain whether the proposed thorium-containing fuel designs are safe in terms of temperature changes and delayed neutron fraction changes during burnup.

In new fuel designs incorporating thorium, when considering the advantages and potential disadvantages of the thorium cycle, including improvements in neutron economy, proliferation risk, and better burn-up, it should be shown that such fuel designs adhere to safety requirements. Van der Walt (2015) has proposed several fuel concepts of in-rod micro-heterogeneous thorium-uranium designs as elaborated in paragraph 4.1.

1.3.2 Objectives

The following steps are taken to reach the objective:

- Conduct a literature survey to assess work done regarding the safety design and operation of PWRs, focusing on the safety features of uranium and thorium fuel.
- Determine a suitable method to evaluate the effect of temperature variation on the reactivity for each proposed fuel design.

- Setup numerical fuel pin models for the Monte Carlo N-Particle (MCNP) Transport Code to simulate the change in k_{eff} with respect to temperature change.
- Assess the safety characteristics of the Th/U fuel designs with regard to reactivity feedback as a function of the temperature of both the fuel and moderator and compare it to uranium-based fuel (as a reference model). The fuel and moderator temperature coefficients of the proposed thorium-containing fuel models will be compared and appraised.
- Compute the delayed neutron fraction of the proposed fuel designs at different burnup points.

  Recommendations for the design and modification of the thorium/uranium fuel design focusing on performance and safety parameters will be made.

2 Theoretical background

2.1 Thorium-based fuel

Thorium is one of the most abundant metallic element in the earth's crust. It is slightly radioactive with higher abundance in acidic rock and granites. Thorium mineral is mostly found in the phosphate mineral called monazite. It was discovered by a Swedish chemist in 1828 Berzelius (René, 2017). The physical properties of thorium in an oxide substance have improved tolerance to high thermal conditions.

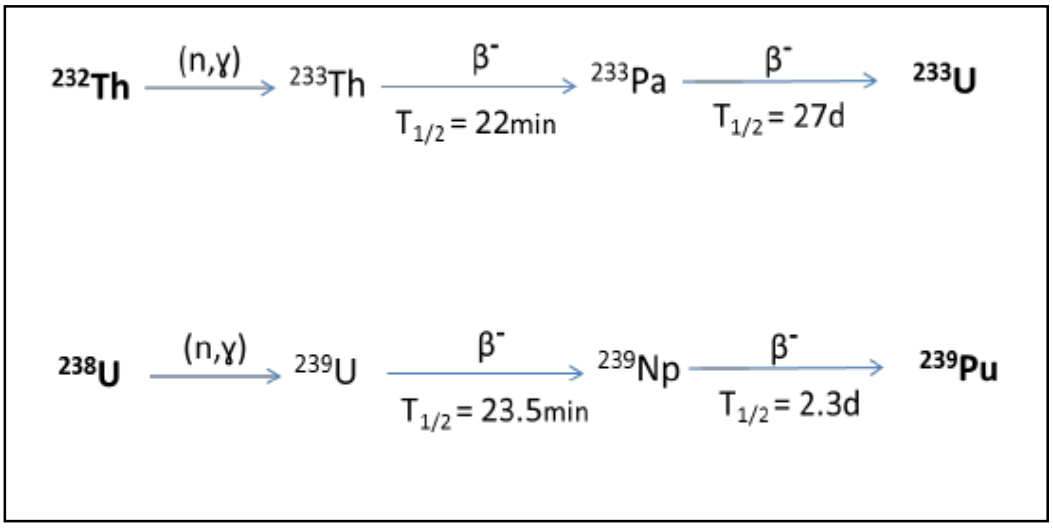

Figure 2-1: Th^{232} and U^{233} fertile-fissile transmutations (Nuclear Energy Agency, 2015)

The thorium and uranium fuel burnup chains are depicted in Figure 2-1. In the thorium cycle, a fertile Th^{232} nucleus captures a neutron to transmute to fissile nuclei: Th^{232} absorbs a neutron to form Th^{233}, which forms Pa^{233} after beta-decay (with a half-life of 2.3 days) and then forms U^{233} after beta-decay (with a half-life of 27 days). Thorium is a fertile material and before significant conversion to U^{233} during burnup, fissile isotopes such as U^{235} or (Pu^{239}) or mixed oxide (MOX) are needed to achieve criticality and excessive reactivity to operate the reactor. U^{238} is fertile and fissionable with fast neutrons and also acts as a fertile element for conversion to plutonium-239 (Das, 2015). The conversion of fissile material Pu^{239} and U^{233}, from U^{238} and Th^{232} respectively, display similar pathways as shown in Figure 2-1. In both cases the process starts with a neutron capture reaction (n, γ), followed by two consecutive beta-decay (β-decay) reactions (Nuclear Energy Agency, 2015). Given significantly longer

half-lives for beta decay in the thorium fuel cycle (in comparison to the uranium cycle), it takes longer to achieve equilibrium of U^{233} than for Pu^{239}. Therefore, a power reactor fuelled by thorium requires fuel material such as uranium oxide (UO_2) at start-up to to have sufficient reactivity available until U^{233} build-up is sufficient to maintain a chain reaction (Dukert, 1970).

If in a conventional reactor fuelled by uranium a long fuel cycle is to be achieved, it would entail using large amounts of enriched fuel. However, that would increase the amount of excess reactivity at the Beginning of Cycle (BOC) which in turn requires a significant amount of neutron absorbers using chemical shim, thus influencing the safety of the reactor (Herring *et al.*, 2001). Thorium has the potential to decrease the excess reactivity at BOC and the advantage of conversion of thorium to fissile material, which would result in an increase the length of the re-fuellin cycle.

2.2 Effect of delayed neutrons

The primary purpose of fission is to generate heat and neutrons to propagate a fission chain reaction. Most of the neutrons produced are emitted instantly when fission takes place. Some neutrons are emitted from fission products through radioactive decay during the fission process. The neutrons emitted promptly at the fission reaction are called, prompt neutrons and account for 99.3% for U^{235} isotope and 99.7% for U^{233} isotope of the neutrons produced during fission, and the rest are delayed neutrons. Different fissile isotopes emit different fission products with characteristic decay chains, resulting in a delayed neutron fraction which changes during burnup. Hence changes in fuel material matrices at reloading and during burnup has an influence on the delayed neutron fraction.

Reactor without delayed neutrons

Consider an infinite critical thermal reactor in which the time between the birth and fission absorption of a neutron is equal to the *prompt neutron lifetime and build-up of fissile* U^{233} denoted by L_p operating without delayed neutrons. Assuming that k_∞ is the multiplication factor and $N_f(t)$ is the number of fissions per cm^3/sec at time t, then the fission rate after L_p seconds will be

$$N_f(t + L_p) = k_\infty \cdot N_f(t) \quad (1)$$

The first term of equation 1 can be expanded as follows

$$N_f(t + L_p) \cong N_f(t) + L_p \cdot \frac{dN_f(t)}{dt}$$

Substituting $N_f(t + L_p)$ back into the equation, the result is

$$\frac{dN_f(t)}{dt} \cong \frac{k_\infty - 1}{L_p} \cdot N_f(t) \quad (2)$$

The solution to the differential equation 2 is

$$N_f(t) = N_f(0) \cdot e^{t/T} \quad (3)$$

Where

$$T = \frac{L_p}{k_\infty - 1} \quad (4)$$

Equation 4 is the reactor period in the absence of delayed neutrons, the period of a reactor is the time required for the neutron level(power) to increase by a factor of e^1. To demonstrate the result of having no delayed neutrons consider k_∞ increasing from 1.000 to 1.001 and where a typical L_p of 10^{-4} secs is specified, then T will be equal to 0.1 secs. Controlling a reactor of that nature, when the rate of change in the neutron population is high, is impossible (Lamarsh and Baratta, 2002).

Reactor with Delayed neutrons.

In a normal reactor, the fission chain reaction is sustained by both the prompt and delayed neutrons. Therefore, the total neutron source in the time-dependant diffusion

equation where prompt neutrons $(1-\beta)$ is the fraction of neutrons that are prompt neutrons and (β) delayed neutrons. Due to fission products being delayed neutron emitters, the rate of decay of the fission products that emit neutrons in the decay process influences the rate of delayed neutron emission.

The time-dependent diffusion and the rate of change of fission products coupled equations are given respectively as

$$L_p \cdot \frac{d\emptyset_T}{dt} = (1-\beta)k_\infty \overline{\sum_a} \emptyset_T + p\lambda C \ - \emptyset_T \qquad 5$$

$$\frac{dC}{dt} = \frac{\beta k_\infty \overline{\sum_a} \emptyset_T}{p} - \lambda C \qquad 6$$

Where $\emptyset_T$ is the thermal neutron flux, C is the fission product concentration, p is the resonance escape probability and λ the decay constant of the precursor.

Equations 5 and 6 are coupled differential equations solved to find $\emptyset_T \ and \ C$ rendering Figure 2-2, which is used to determine the reactor period (Lamarsh and Baratta, 2002).

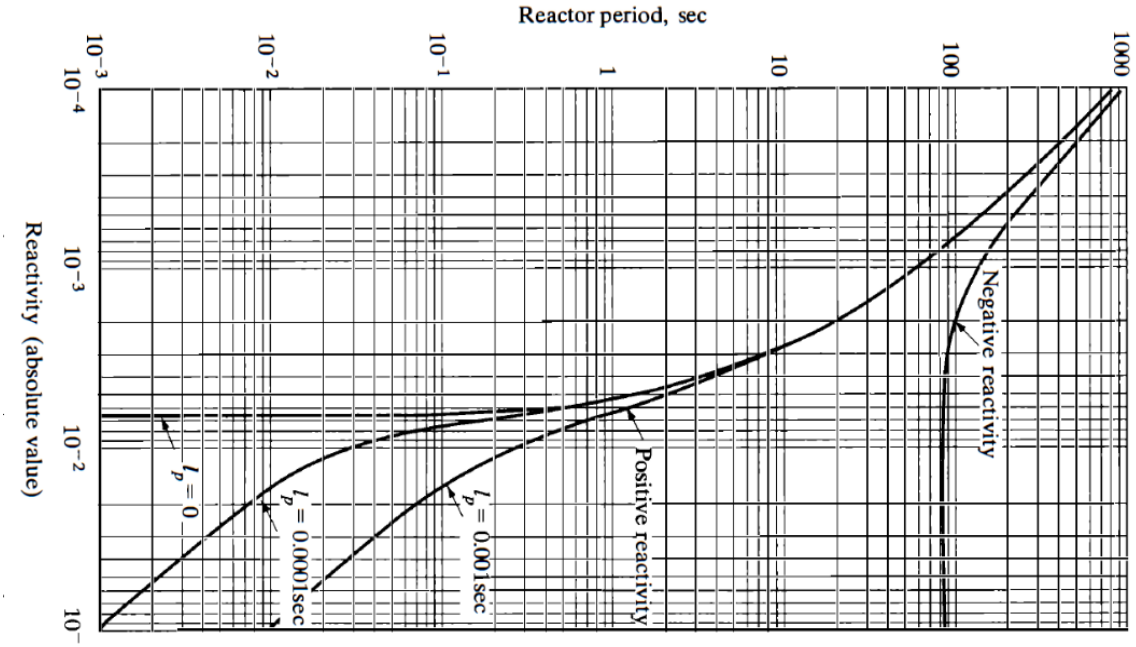

Figure 2-2: Reactor period vs reactivity for a U^{235} fuel (Lamarsh and Baratta, 2002)

Using Figure 2-2 to determine the influence of delayed neutrons, consider k_∞ increasing from 1.000 to 1.001, with L_p equal to 10^{-4} secs and the reactivity is equal to 10^{-3}. From Figure 2-2 reactor period is approximately equal to 58 seconds. Therefore, the time required to control the reactor is increased when delayed neutrons are present (Lamarsh and Baratta, 2002).

Delayed neutron fraction

A prompt critical state is when the reactor is in a critical state due to prompt neutrons only, that is, the reactivity is equal to the delayed neutron fraction. In order to control the reactor, the excess reactivity should be less than the delayed neutron fraction. Each fissile isotope has a different β_{eff} associated with it. As depicted in Figure 2-3, U^{235} has a higher β_{eff} compared to other fissile isotopes. Therefore, the delayed neutron fraction is influenced by the fuel material composition, that is, during burnup β_{eff} changes as the fission products build up. In a conventional uranium fuelled reactor, at BOC β_{eff} is high and decreases as the fuel burns up resulting in a lower β_{eff} at EOC, this occurs due to the production of Pu^{239}. Similarly, a thorium/uranium fuelled reactor β_{eff} at BOC is greater than that at EOC due to the build-up of U^{233}. Therefore, it is highly important when introducing thorium/uranium fuel that a safety characteristic analysis is done to determine if the fuel design falls within the licenced safety margin.

Nuclide	β (thermal neutron fission)	β (fast fission*)
^{232}Th	—	0.0203
^{233}U	0.0026	0.0026
^{235}U	0.0065	0.0064
^{238}U	—	0.0148
^{239}Pu	0.0021	0.0020

*Fission induced by prompt neutron spectrum.

Figure 2-3: Delay neutron fraction of fissile isotopes (Lamarsh and Baratta, 2002)

2.3 Temperature effects on reactivity

When fission takes place inside a fuel pin, energy is released in the form of heat. Due to the temperature difference between the fuel pin and the coolant, transfer of energy from the fuel to the coolant takes place, i.e. from a higher temperature heat source to a lower temperature heat sink. The temperature change affects the core's effective multiplication factor. This change results in reactivity change which plays an important role in the safe operation of the reactor. The Temperature Coefficient of Reactivity α_T is a parameter that is used to analyse the effect of temperature on reactivity. It is defined as the derivative of the core reactivity ρ with respect to temperature T.

$$\alpha_T = \frac{d\rho}{dT} \qquad 7$$

The following equation defines ρ with respect to multiplication factor k,

$$\rho = \frac{k-1}{k} \qquad 8$$

Substituting equation 8 into 7 and differentiating equation 11 results with

$$\alpha_T \approx \frac{1}{k} \cdot \frac{dk}{dT} \qquad 9$$

The algebraic sign of α_T (the temperature coefficient) determines the response of a reactor to temperature change. When α_T is positive, the increase in temperature results in an increase in reactivity and the opposite when it is negative. An increase in reactivity can lead to fuel a sudden heat up of the fuel that eventually may result is physical damage to the fuel if fuel coolant systems fail and if no interventions are made. If the reactor has a negative α_T an increase in temperature leads to a decrease in reactivity, thus decreasing the amount of energy produced. Therefore, negative temperature feedback both in the fuel and moderator (for a water-cooled thermal reactor) is essential in keeping the reactor stable. When designing a reactor the fuel

temperature coefficient (α_{TF}) and moderator temperature coefficient (α_{TM}) are required to be negative for a safe, inherently stable reactor (Lamarsh and Baratta, 2002).

Fuel Temperature Coefficient

Temperature variation affects the neutron absorption in the resonance region of the nuclide cross-section. When the temperature of the fuel increases, the width of the resonance peaks increases, due to the Doppler Effect, resulting in an increase in neutron absorption in the resonance region, thereby decreasing the resonance escape probability factor (*p).* Figure 2-4 shows that as the temperature of the fuel rises the resonance cross-section widens and becomes less peaked (exemplified for U^{238} nuclei).

The change in the shape of the resonance is referred to as Doppler broadening. The area under the curves remains constant for all temperatures, therefore as the temperature increases, the number of neutrons captured increases, thus decreasing the number of thermal neutrons (Lamarsh and Baratta, 2002).

The fuel temperature coefficient of reactivity is calculated in terms of the resonance integral (I):

$$\alpha_{TF} = \frac{1}{k} \cdot \frac{dk}{dT_F} = \ln p \cdot \frac{1}{I} \cdot \frac{dI}{dT_F} = -\ln\left[\frac{1}{p(300K)}\right] \cdot \frac{\omega_F}{2 \cdot \sqrt{T_F}} \qquad 10$$

Where ω_F is a constant which depends on the fuel composition and p is resonance escape probability factor.

Moderator Temperature Coefficient

The change in temperature of reactor coolant affects the coolant density, which influences reactivity due to a change in moderation and neutron absorption. Increasing the temperature of the moderator decreases the coolant density which results in expansion of the fluid. The reduction in coolant density results in two competing

effects, namely loss in moderation and (when boron is still present in the coolant) increase in thermal utilisation due to an effective reduction in boron concentration.

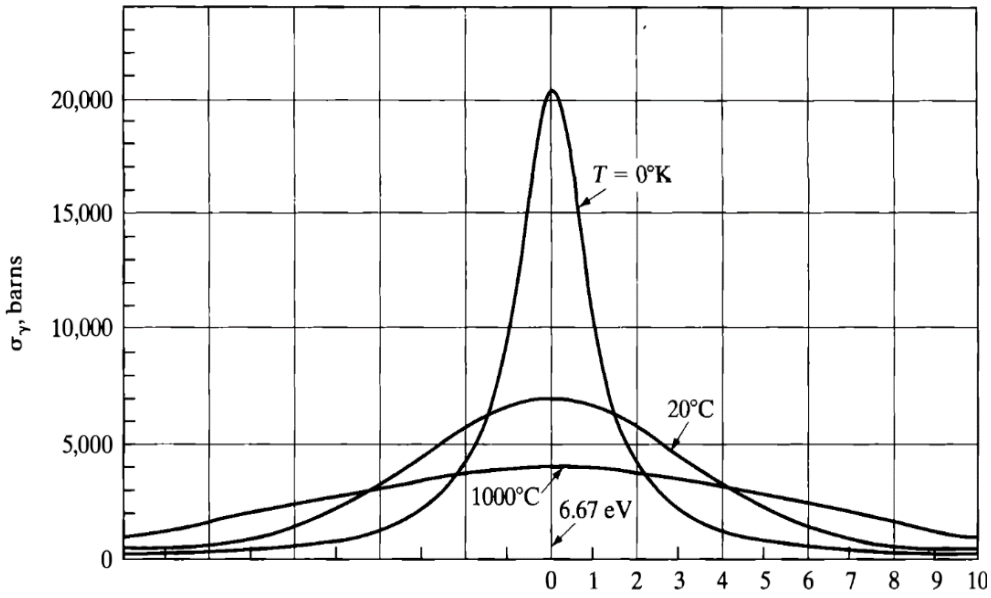

Figure 2-4: Doppler-broadening of the absorption resonance of U-238 at 6.67eV (Lamarsh and Baratta, 2002)

Coolant expansion at constant pressure reduces neutron moderation, thus decreasing the multiplication factor, contributing to a negative MTC. This effect dominates in the absence of high soluble boron concentrations, typically sometime after BOC. However, if at BOC boron concentration is high, increasing the coolant temperature (and hence a decrease of the density of coolant) results in a reduction of soluble neutron poison (boron) density leading to a reduction in neutron absorption. This effect adds reactivity to the core. It is important that at BOC the addition of reactivity due to higher moderator temperature in the presence of soluble boron does not dominate the removal of reactivity stemming from reduced thermalisation hence the level of boron concentration has to be within limits. Burnable absorbers in the fuel are typically used when excess reactivity is not sufficiently limited by control rods and chemical shim – typically in fresh fuel loads and are also used for flux flattening purposes. The *thermal utilization factor* increases due to a decrease in neutron absorption in the boron, resulting in a positive MTC. As indicated in Figure 2-5 an increase in the boron concentration in the moderator contributes to a more positive MTC for the reactor (Lamarsh and Baratta, 2002).

For a thermal water-cooled reactor, MTC is a function of the *thermal utilization factor f and resonance escape probability factor p* due to the density and temperature variation of the moderator. The MTC is expressed as

$$\alpha_m = \alpha_m(\overline{T_f}) = \frac{1}{k_\infty}\frac{\partial k_\infty}{\partial \overline{T_m}} = -\theta_m\left[\ln\left(\frac{1}{p}\right) - (1-f)\right] \quad 11$$

Where θ_m is the volumetric coefficient(Lewis, 2008).

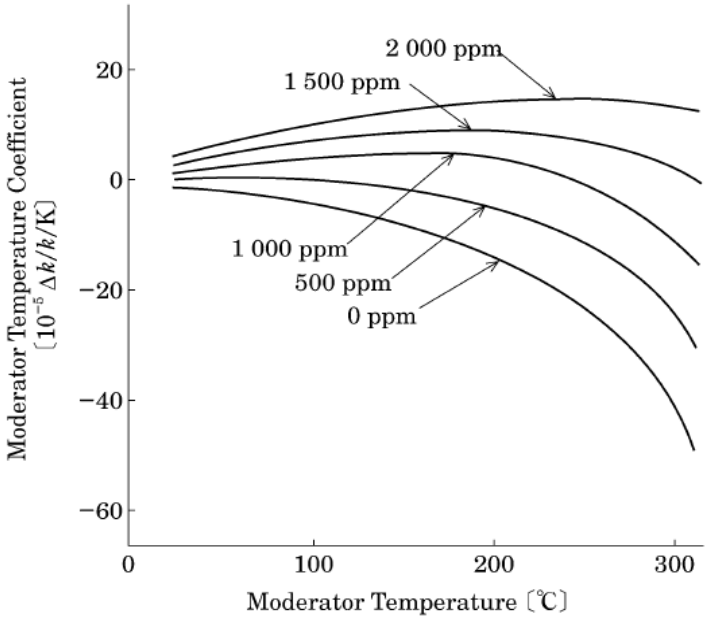

Figure 2-5: Moderator Temperature Coefficient vs Temperature for different Boron concentration (Oka, 2014)

3 Literature review

3.1 Heterogeneous thorium fuel designs

The growing interest in the use of thorium in PWR and other reactor types, at many research institutes, is attributable to several advantages of using thorium in nuclear reactors, such as, to name a few, the abundance of ore deposits, the production of fissile isotopes (transmutation) during burnup and better thermal conductivity properties thus improving heat transfer in the fuel. These advantages far outweigh possible disadvantages, which include the need for inclusion of fissile isotopes at BOC (to achieve criticality for production of U233 through Th232 transmutation) and a lower delayed neutron fraction (which reduces the delayed neutron fraction in case of heterogeneous thorium fuel design

Du Toit and Cillers (2014) investigated the economic benefits of a thorium-uranium once-through homogeneous mixed fuel run in a 24-month fuel cycle in a PWR and compared it to a once-through uranium cycle. The comparison focused on the operational savings obtained due to the use of Th^{232} which leads to longer fuel cycles. This in turn provides a reduction in downtime from fuel loading, resulting in increased plant performance. However, it should be noted that the need for high uranium enrichment for a once-through Th-U cycle increased the initial cost of fuel in the initial cycle.

Serfontein and Mulder (2014) compared the fuel economy and the proliferation risk between thorium and uranium cycles. A theoretical appraisal of the resonance integrals and fast fission cross-sections of Th^{232} compared to U^{238}, rendered a U/Pu fuel cycle with a higher conversion potential in the fast neutron energy spectrum compared to the U/Th fuel cycle due to the better neutronic properties of U^{233} (than U^{235}) converted from Th^{232}. Electricity production cost in a uranium cycle is lower than that in a thorium cycle due to the need for reprocessing spent thorium fuel. The researchers found the Th-cycle to be not cost-effective. Due to high levels of radiation by U^{232} access to U^{233} is deprived thus increasing proliferation resistance for the U/Th cycle. On the other hand, Serfontein and Mulder concluded that U^{233} can be accessed by using chemical separation before a significant build-up of U^{232}.

Du Toit and Naicker (2018) studied the neutronic behaviour of an EPR with a 24-month thorium/uranium cycle design using MCNP6. The original uranium EPR fuel contained Gd_2O_3 in the fuel pin. Replacement of Gd_2O_3 and UO_2 with ThO_2 in certain sections of the fuel pin was performed without altering the geometry of the fuel design. The build-up of Xenon and Samarium fission products for Th-B1(thorium-based) fuel assembly is lower resulting in improved burnup compared to the original U-B1(uranium-based) fuel assembly. Furthermore, a lower rate of fissile depletion was found for the Th-B1 fuel assembly resulting in increased burnup and hence an increase in the fuel cycle. The delayed neutron fraction at end of cycle is smaller for the Th-B1 fuel assembly than the U-B1 fuel assembly which warrants careful consideration in terms of reactor safety and control.

3.2 Reactivity temperature coefficient

3.2.1 Uranium MOX fuel

Dawahra *et al*. (2016) performed an analysis of the reactivity temperature coefficient of a Miniature Neutron Source Reactor (MNSR) for normal and transient operational conditions using HEU (UAl_4) and LEU (U_3Si, U_3Si_2 and U_9Mo). The normal and transient operational conditions were set to calculate FTC, by varying the fuel temperature and controlling the moderator temperature and coolant density. The moderator temperature and density were varied to calculate MTC for comparison with previous similar literature studies. The calculated FTC for LEU rapidly becomes more negative as the temperature of the fuel increases from 20^0C to 40^0C, whilst HEU has a less negative value of the FTC. This occurs due to LEU fuel having more U-238, resulting in a higher increase in resonance absorption compared to HEU fuel. The MTC for HEU (UAl_4) and LEU (U_3Si_2) is negative between 20^0C and 40^0C, however, U_3Si and U_9Mo have a positive MTC at temperatures up to 40^0C and have a negative MTC at temperatures above 70^0C.

Alhassan *et al.* (2010) investigated the FTC and MTC of the LEU (UO_2) fuel pin model which is under development and a reference fuel pin model HEU (UAl_4). The analysis was carried out using a FORTRAN-95 code. The temperature conditions were simulated at BOC with a temperature range between 15^0C to 140^0C. The total

temperature coefficient of reactivity shows that LEU has a positive coefficient in comparison to the HEU which is negative between 50^0C and 140^0C. On the other hand, FTC and MTC for both the fuel pin models are negative, however, HEU has a more negative value in comparison to LEU. For the purpose of LEU being investigated for replacing HEU, Alhassan *et al.* (2010) conclude that LEU should replace HEU, however, more investigation is required to evaluate the overall temperature coefficient of reactivity with a thermal-hydraulic code coupled to neutronics.

Pinem *et al.* (2018) performed an analysis of changes in the fuel and moderator temperature against reactivity and further evaluated the effect of changes in boron concentration and moderator density for an AP1000 PWR core. A NODAL3 code is utilized to calculate the effective multiplication factor at different temperatures without the presence of control rods. Input data such as absorption macroscopic cross-section, diffusion coefficient, group scattering cross-section, boron concentration and fission spectrum were calculated with the SRC code. All the reactor core design parameters were based on the AP1000 report. To calculate FTC at different fuel temperatures, the moderator and cladding temperatures were kept constant at 600K. Cross-sections were generated using SRAC code for temperatures between 573K and 1273K. To calculate the MTC, cladding and fuel temperatures were kept at 600K and 900K respectively. The calculation results indicate that FTC and MTC are in the range of -2.613 pcm/^{0}C to -4.657 pcm/^{0}C, and -1.00518 pcm/^{0}C to 1.00649 pcm/^{0}C respectively. The study showed that both FTC and MTC of the reactor are negative and that adding boron to the moderator makes the FTC more negative and makes the MTC less negative. A less negative MTC indicates that as the moderator temperature increase so does the reactivity, this leads to heat generation which reduces the moderator density affecting the moderator effect and fuel cooling. Therefore, the transient analysis requires attention to MTC in the range between 20^0C - 90^0C.

3.2.2 Thorium heterogeneous fuel

Tucker, Alajo and Usman (2015)noted that thorium and plutonium mixed oxide as fuel for PWR addresses issues related to thorium is an abundant mineral which is not in use by the nuclear industry. Therefore, a feasibility study at steady-state BOC conditions was done to compare a 100% UO_2 core and 2/3 UO_2 & 1/3 Th-Pu fuel core.

The temperature coefficient of reactivity was investigated among other parameters between a 100% UO_2 and a mixed oxide core. To determine the temperature coefficient, three MNCP models were created for both fuel cores. The first simulation was performed with cross-sections at room temperature of the fuel and coolant, and a coolant density of 1g/cm^{3}and the second simulation was performed with cross-sections at room temperature of the fuel and coolant, and a coolant density of 0.711g/cm^3. The third simulation cross-section temperature was at 600K for fuel and 293.6K for the coolant. The total temperature coefficient for the UO_2 fuel was positive; it was however negative for the mixed oxide. Both the FTC for UO_2 and Th-Pu was negative.

Using reactor safety and performance parameters such as fuel cycle length, reactivity coefficient and thermal safety margin, Gorton *et al.* (2019) compared three different Thorium mononitride & Uranium mononitride (ThN-UN), Uranium mononitride (UN) and UO_2 fuel designs. The study aimed to understand the benefits of non-proliferation waste and accident tolerance characteristics displayed by ThN-UN as a fuel. A two-dimensional PWR fuel pin cell was modelled in MPACT (which is a Monte Carlo deterministic code for LWRs) based on an AP1000 reactor core geometry design. The results showed that FTC for each of the above-mentioned fuels was negative for the whole cycle, however, UO_2 had a less negative FTC compared to the rest of the nitride-based fuels including UN due to an increased fuel density in the nitride-based fuel and increased absorption from U-238 and Th-232. The moderator-to-fuel ratio for nitride fuel was greater than that of UO_2 due to increased heavy metal loading which contributed to moderation[1], thus MTC for ThN-UN & UN fuel was more negative in comparison to UO_2. In the presence of boron, the MTC of the fuel indicates that an increase in boron results in MTC being less negative. In closing, Gorton *et al.* (2019), stated that ThN-UN mixtures are a feasible fuel for use in PWRs under normal operational conditions.

Zainuddin, Parks and Shwageraus (2016) investigated the factors contributing to a positive MTC for a Pu-Th fuelled PWR and further identified burnable poisons which

[1] Due to the high thermal conductivity properties of mono-nitrides, the rate of heat transfers from the fuel (containing mono-nitrides) to moderator is greater, which leads to increase in coolant temperature, thus contributing to coolant thermal expansion.

could help in mitigating positive MTC. Due to high Pu content that leads to too much excess reactivity, it was assumed that a positive MTC was a result of a large boron concentration to reduce excess reactivity. However, with an average boron concentration of 1600ppm for both fresh and depleted fuel, the main contribution to a positive MTC is the increased fission in the epithermal range by Pu^{239}, Pu^{241} and U^{233}. Therefore, from the study, it was evident that the type of fuel using plutonium instead of uranium contributed to a positive MTC. The level of boron concentration has less influence on the excess reactivity, thus a suitable burnable poison was required to manage MTC.

Uguru *et al.* (2021) studied the neutronic and safety parameters of a Th-U mixed oxide fuel cycle in a small modular reactor. The reactor core is partitioned into three enrichment zones with the middle and highest enriched fuel zones containing burnable neutron absorbers. To perform a criticality calculation MCNPX was coupled with CINDER90. The K-code calculations indicated that the k_{eff} value decreased with an increase in fuel temperature due to a decline in fission reactions which are due to the neutron spectrum hardening. Furthermore, a reactor core with fewer U^{235} will have the lowest k_{eff} value. The MTC and FTC for all six different cores became less negative as the temperature of the moderator and fuel respectively decreased. The MTC value fell within the design value (0 pcm/K to -40pcm/K) of the UO_2 AP1000 reference model, while the FTC ranged between -3.5pcm/K and -1.3pcm, which was within and above the reference model design value of -2.1pcm/K to -1.0pcm/K. It was concluded that the core with the lowest enrichment provided better results, thus it was used to perform burnup calculations.

3.2.3 Effects of neutron poisons

Minor actinides are neutron poisons which are typically found in spent fuel. Liu *et al.* (2018) investigated the effect of adding minor actinides in an AP1000 core by coating minor actinides with layers of different thicknesses on the fuel pellets. A few minor actinide loading patterns were proposed to calculate k_{eff} with the variation of minor actinide loading quantity. Loading patterns with the least and highest amounts of minor actinides had the lowest and highest k_{eff} respectively. Loading patterns with 4.45% U^{235} enrichment had the least impact on the k_{eff} value, thus it was used to perform the

FTC and MTC calculations. A comparison between a core with and without minor actinides was done for the temperature coefficient of reactivity. Adding minor actinides indicated that a negative MTC and FTC were achieved. The FTC and MTC became less negative as the temperature of the fuel increased with a steep gradient.

Uguru *et al.* (2020) investigated the effect of boron in the light-water moderator and gadolinium in the fuel on the neutronic properties of ThO_2-UO_2 fuel in a small modular reactor using the MCNP code integrated with CINDER90. A comparison was done between four fuel assemblies as follows: one without boron in the moderator and gadolinia in the fuel; one with boron in the moderator without gadolinia in the fuel and the other two assemblies contained both boron in the moderator and gadolinia in the fuel at different concentrations. The calculation at BOC showed that adding boron reduced excess reactivity and the addition of burnable poisons in the fuel also reduced excess reactivity. Viewing the MTC of a core without boron and with boron, showed that adding boron makes MTC less negative and the MTC for a UO_2 -fuelled AP1000 reactor is less negative compared to an MTC of Th-UO_2 fuel due to fuel type. On the other hand, the presence of boron decreases the FTC with temperature change due to increased neutron absorption and therefore hardening of the neutron spectrum.

Hafez *et al.* (2021) performed criticality calculations of a PWR VVER-1200 at the first and second phases of the initial fuel loading in cold, hot and normal states. The MCNP5 transport code was used to calculate the eigen value to determine the effect of different boric acid concentrations and the variation of the coolant temperature and density. Criticality analyses were done in a cold state with moderator temperature at 20^{o}C and a hot state with the coolant temperature set at 32^{o}C. The effective multiplication factor was calculated for a core with and without boric acid in the coolant for cold and hot states respectively. The comparison between the two cores indicated that introducing boric acid reduces k_{eff} due to the high absorption cross-section of B-10 in H_3BO_3 at thermal neutron energy. However, at high temperatures (hot-state) the effect of boron is less than at lower temperatures (cold-state). The researchers performed criticality calculations of the core at three conditions with different boric acid concentrations in the moderator, and point out that at high boron concentrations in a hot state, increasing temperature results in k_{eff} increasing and consequently leading to a positive temperature coefficient of reactivity, which is not acceptable from a reactor

safety point of view. The paper revealed that boron concentration limits during operation are significant in preventing unstable reactor operation.

4 Methodology

The majority of operating nuclear reactors in the world are of the PWR type; 302 out of 442 operating nuclear reactors in the world are PWR (IAEA, 2021). The need for improving the design and operational parameters for a PWR contributes to the improvement of the efficiency and safety of the nuclear reactor, particularly power reactors. Among those parameters is the fuel cycle length which is influenced by the physical and neutronic properties of the fuel material and the design systems and sub-system of the reactor[2]. Typical PWRs use uranium oxide as a fuel which is enriched to less than 5% U^{235} fuel content. Different methods of improving fuel cycle length have been proposed in the literature and include the use of thorium-uranium fuel. Van der Walt (2015) proposed a heterogeneous thorium-based fuel for a PWR to increase fuel cycle length. The fuel comprises ThO_2 pellets and UO_2 pellets of different pellet lengths, in a ThO_2-UO_2 sequence over the entire fuel rod length, and is intended to create conditions for optimal transmutation of Th^{232} to U^{233}.

The above-mentioned proposed heterogonous fuel designs were modelled in a Monte-Carlo neutronic simulation as described below to study the effect of varying the moderator and fuel temperature, respectively, for each fuel design. Criticality calculations were performed to simulate the effect of varying temperatures using the MCNP and SERPENT software to determine the reactivity and temperature coefficient of both the fuel and moderator and to determine the influence of burnup on the fraction of delayed neutrons. The first calculation focuses on the fuel pin model of the proposed fuel designs using MCNP at the following burnup points, that is, BOC, MOC and EOC to calculate k_{eff}. Section 4.2 describes the method to determine k_{eff} using MCNP. The second calculation focuses on the full core of the proposed fuel design at BOC burnup point to determine k_{eff} using SERPENT as described in Section 4.4.

[2] This includes the design of components making up the thermal & fluid-flow systems, strength analysis, control systems among others.

4.1 Material and geometry description

The numbers in Figure 4-1 and Figure 4-2, correspond to the specified materials and parts as indicated below:

1. Fuel: ThO_2
2. Helium filled gap between fuel and cladding.
3. Zircalloy-4 cladding.
4. Water is the coolant/moderator.
5. Fuel: UO_2

Three proposed heterogeneous thorium-uranium fuel designs and a uranium oxide reference fuel design were considered in this project. Each thorium-uranium fuel design comprises ThO_2 and UO_2 pellets, with different lengths and different UO_2/ThO_2 ratios, all with equal radii. The reference fuel model only contains UO_2 pellets. The first fuel design, denoted 1Th1U, comprises 1cm length ThO_2 pellets and 1 cm length UO_2 pellets, the second fuel design denoted 3Th1U comprises 3cm length ThO_2 pellets and a 1cm length UO_2 pellets, and the third fuel design comprises 5cm ThO_2 pellets and 1cm length UO_2 pellets.

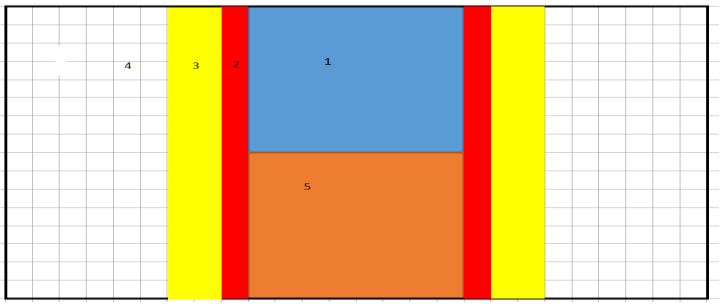

Figure 4-1: Side view of the proposed fuel design model

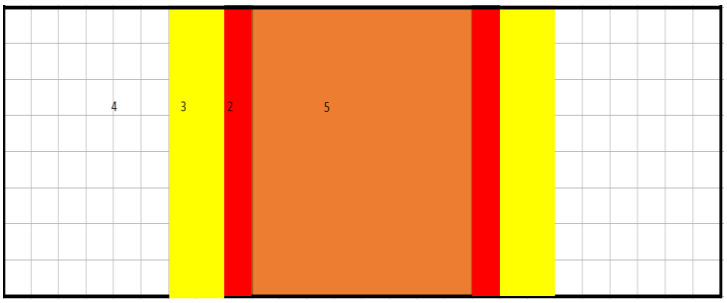

Figure 4-2: Side view of the reference fuel

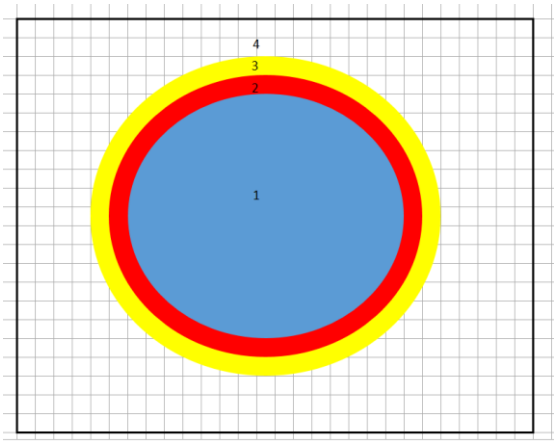

Figure 4-3: Axial view of the proposed fuel design model

To model an equilibrium fuel pin and full-core, each fuel design contains fresh, once burned, and twice burned thorium and uranium fuel respectively. A once-burn fuel refers to fresh fuel that has completed one burnup cycle before fuel refuelling and a twice-burn refers to fresh fuel that has completed two burnup cycles before fuel reloading. Each fuel design model included simulations without boric acid in the coolant for fuel temperature change and moderator temperature change effects. To determine the effects of the presence of boric acid due to temperature change on reactivity, each fuel design model was simulated for moderator temperature change in the presence of boric acid at various concentrations, as described below.

4.2 Numerical simulations and procedure

4.2.1 Use of numerical models

The use of computational models in this study enables simulation of the proposed fuel design without physically testing the designs. Simulations can be done within a short period and save costs. With the aim of understanding the behaviour of reactivity effects due to temperature changes in the moderator and fuel, the proposed designs are not intended for physical testing and therefore further research on the material strength and thermodynamic behaviour is essential to ensure the safety and practical application.

The MCNP6 (Monte Carlo N-Particle) code is recognised as a highly-accurate industry-standard software code, one of a series of Monte Carlo transport codes

developed at the Los Alamos National Laboratory and is widely used by researchers. MCNP6 was used to perform criticality calculations.

The computational model simulates a fuel rod and surrounding material such as Helium gap, cladding material and moderator respectively, enclosed within a specified geometry. The cell card in input files contain important design parameters such as material density, volume and temperature. In addition, isotope continuous-energy cross-sections are specified.

4.2.2 Numerical procedure

The numerical procedure in this project refers to the methods that were used to calculate the FTC and MTC for each proposed fuel design and the reference fuel pin design. A standardised and consistent method of editing the input files for each proposed new fuel design and the reference fuel was considered. The form of the equations for fitting curves to simulated data is based on the theoretical functions for determining FTC and MTC.

Input files: Fuel Temperature Change

Input files to perform a criticality calculation for change in fuel temperature were done at temperatures of 300K, 600K, 900K and 1200K, which coincide with the continuous-energy cross-sections indicated in the material specification libraries are 80c, 81c, 82c and 83c respectively. The temperature and cross-sections were applied correctly in the cell and material card sections. The temperature of the Helium gap, fuel cladding and moderator was chosen to remain constant at 900k, 800k and 650k, respectively. Figure 0-1 and Figure 0-2 show the cell card and material cards, respectively, of the input file for fuel temperature at 300K in the Annexures.

Input files: Moderator temperature change without boric acid, with 1000ppm boric acid and boron at different concentrations

Input files to perform KCODE calculations for change in moderator temperature were done at 550K, 560K, 570K, 580K, 590K and 600K respectively. The MCNP continuous-energy cross-section file for each fuel simulation is designated as 81c in

the material cards, which corresponds to a temperature of 600K, which is the closest temperature for which the ENDF/B-VII.1 library contains continuous energy cross-sections needed for the simulation. The temperature of the Helium gap and fuel cladding was specified to be constant at 900K and 800K respectively. The Uranium fuel temperature was specified at 1200K and for thorium at 1000K. All parameters in the simulation setups for the above-mentioned moderator temperature change conditions, and thus the specified material cards, were identical, except the material card which specifies the moderator material cross-sections Figure 0-3 and Figure 0-4 show the cell card and material cards respectively, of the input file for moderator temperature at 550k in the Annexures.

Input files: Determining delayed neutron fraction

The delayed neutron fraction was determined by applying the prompt method, where two MCNP KCODE simulations are done to find the k_{total} (effective multiplication factor considering the presence of the prompt and delayed neutrons) and k_{prompt} (effective multiplication factor considering the presence of the prompt neutrons). Equation 4.1 was used to calculate the delayed neutron fraction.

$$\beta_{eff} \cong 1 - \frac{k_{prompt}}{k_{total}} \qquad 4.1$$

The input file for the reference fuel model and three proposed designs have the same input file with the input file for fuel temperature change at 1200K. Therefore, the k_{total} value was taken from the fuel temperature change simulations for all the fuel models. The input file to calculate k_{total} has no TOTNU Data Card. The TOTNU Data Card prevents the influence of delayed neutrons when performing KCODE calculations, therefore, the effective multiplication factor calculated accounts for prompt neutrons only.

4.3 Method of analysis

For each of the proposed fuel designs and reference fuel of an equilibrium fuel model, three burnup positions were calculated, namely BOC, MOC and EOC. For each

burnup position listed, the fuel temperature was varied from 300K to 1200K with 300K intervals and the moderator temperature was varied between 550K and 600K with temperature steps of 50K. However, each moderator temperature change was done for three conditions, namely, with no boron, at a 1000ppm boron concentration and by varying boron concentration such that the simulation rendered a k_{eff} within the 1.048 to 1.052 range[3].

Table 1: Data tabulated from MCNP simulation

Fuel design: 1Th1U			
Fuel Temperature Coefficient			
Temperature(K)	**K_{eff}**	**ρ**	**α_F**
300	1,2119	0,1749	
600	1,1904	0,1599	-1,49E-04
900	1,1774	0,1507	-9,25E-05
1200	1,1660	0,1424	-8,33E-05
Average	1,1864	0,1570	-1,08E-04

The k_{eff} results from the simulations were used to calculate the reactivity and temperature coefficient of reactivity as a function of temperature, from which reactivity, FTC, and MTC curves respectively were directly obtained. A curve-fit was obtained for the reactivity curve to remove variability. The function obtained for curve-fitting (see section 4.3.1 below), which is reactivity as a function of temperature, was differentiated to obtain FTC and MTC as a function of temperature. Table 1 shows MCNP simulated data showing multiplication factor, reactivity and temperature coefficient. Table 2 provides an output summary of the k_{eff}, reactivity and temperature coefficient of reactivity obtained from the derived equations. Equation 4.7 below was used to calculate the k_{eff}

[3] The range was chosen arbitrarily, the approach to render comparable results is the same for all models and furthermore the range was chosen to reduce computational time.

Table 2: Tabulated data of reactivity, k_{eff} and temperature coefficient of reactivity[4]

Fuel design: 1Th1U					
Fuel Temperature Coefficient					
$\boldsymbol{\rho}$	$\boldsymbol{\alpha_F}$	$\mathbf{k_{eff}}$	**a**	**b**	**T(K)**
1,742E-01	-5,280E-05	1,2110	0,79470	0,00222	300
1,610E-01	-3,793E-05	1,1919	0,79470	0,00222	600
1,507E-01	-3,135E-05	1,1774	0,79470	0,00222	900
1,419E-01	-2,743E-05	1,1654	0,79470	0,00222	1200

4.3.1 Deriving the k_{eff} equation and curve-fit approximation function for the FTC and MTC.

The best-fit curve equation is fitted into the calculated k_{eff} as a function of temperature data points from the simulation which represent the form of the function that defines the effect of temperature on reactivity.

The four-factor formula multiplication factor is defined by Equation 4.2:

$$k_{eff} = \eta \cdot \varepsilon \cdot p \cdot f \cdot P_F \cdot P_T \qquad 4.2a$$

Where ε is the fast fission factor , η is the average number of neutrons emitted per thermal neutron absorbed, p is the resonance escape probability factor, f is the

[4] Equation 4.9 is α_T as a function of temperature and constant “a” & “b”

thermal utilization factor, P_F is the fast neutron leakage factor and P_T is the thermal neutron leakage factor (Lamarsh and Baratta, 2002).

For the purpose of determining the temperature dependency of k_{eff}, p is considered to be temperature dependent[5] while $\eta, \varepsilon \; and \; f$ are treated as temperature independent constants in the curve-fitting exercise.

Therefore, if $\eta \cdot \varepsilon \cdot f \cdot P_F \cdot P_T$ in Equation 4.2 is defined as constant C_1, k_{eff} can be written as

$$k_{eff} = C_1 \cdot p \qquad 4.2b$$

The resonance escape probability factor p is defined by Equation 4.3:

$$p = exp\left(-\frac{N_F \cdot V_F}{\zeta_M \cdot \sum_{sM} \cdot V_M}.I\right) \qquad 4.3$$

Where $V_M \; and \; V_F$ are the volumes of the moderator and fuel, respectively, ζ_M is the moderator slowing down decrement, N_F is the fuel atom density, $\sum_{sM}$ is the moderator macroscopic scattering cross-section and I is the resonance integral (Lamarsh and Baratta, 2002).

In Equation 4.3 the resonance integral I is a function of temperature and $\frac{N_F \cdot V_F}{\zeta_M \cdot \sum_{sM} \cdot V_M}$ is temperature independent. Therefore $\frac{N_F \cdot V_F}{\zeta_M \cdot \sum_{sM} \cdot V_M}$ can be considered to be a constant C_2.

Thus, Equation 4.3a can be written as:

$$p = exp(-C_2.I) \qquad 4.3b$$

[5] In fuel temperature coefficient determination it is assumed as a valid approximation that p is considered as a dominating temperature dependent factor in Doppler broadening.

The resonance integral I is defined as:

$$I = I_o \cdot \left[1 + \varphi_a\left(\sqrt{T} - \sqrt{I_o}\right)\right] \quad 4.4a$$

Where T is the temperature and the parameter φ_a is a function of the surface of the mass ratio of the fuel element which is a constant, respectively. I_o is the absolute resonance integral at the absolute temperature of 300K (Lamarsh and Baratta, 2002; Lewis, 2008)

Simplifying Equation 4.4a renders:

$$I = I_o \cdot \left[1 + \varphi_a\left(\sqrt{T} - \sqrt{I_o}\right)\right] \quad 4.4a$$

$$I = \left(I_o - \varphi_a \cdot I_o \cdot \sqrt{I_o}\right) + \varphi_a \cdot I_o \cdot \sqrt{T} \quad 4.4b$$

From Equation 4.4b, $\left(I_o - \varphi_a \cdot I_o \cdot \sqrt{I_o}\right)$ and $\varphi_a \cdot I_o$will be defined as C_3 and C_4 respectively, where C_3 and C_4 are constants. Therefore, Equation 4.4b gives:

$$I \cong \mathrm{C}_3 + \mathrm{C}_4 \cdot \sqrt{T} \quad 4.4c$$

Substituting Equation 4.4c into Equation 4.3 results in:

$$p = exp\left(-\mathrm{C}_2.\left(\mathrm{C}_3 + b \cdot \sqrt{T}\right)\right) \cong e^{-\mathrm{C}_2\left(\mathrm{C}_3 + \mathrm{C}_4\sqrt{T}\right)} \quad 4.5$$

Substituting Equation 4.5 into Equation 4.2b result in Equation 4.6 which is a good approximation for the four-factor formula:

$$k_{eff} \cong \mathrm{C}_1 \cdot e^{-\mathrm{C}_2\left(\mathrm{C}_3 + \mathrm{C}_4\sqrt{T}\right)} \cong \left(\mathrm{C}_1 \cdot e^{-\mathrm{C}_2}\right) \cdot e^{-\mathrm{C}_2 \cdot \mathrm{C}_4\sqrt{T}} \quad 4.6$$

The temperature coefficient of reactivity is a function of the reactivity derivative with respect to temperature. Reactivity is defined as:

$$\rho = 1 - {k_{eff}}^{-1} \qquad 4.7$$

Substituting Equation 4.6 into Equation 4.7 results in

$$\rho = 1 - \left[(\mathrm{C}_1 \cdot e^{-\mathrm{C}_2}) \cdot e^{-\mathrm{C}_2 \cdot \mathrm{C}_4 \sqrt{T}}\right]^{-1} = 1 - \frac{e^{\mathrm{C}_2 \cdot}}{\mathrm{C}_1} \cdot e^{\mathrm{C}_2 \cdot \mathrm{C}_4 \sqrt{T}} \qquad 4.8a$$

Defining $\frac{e^{\mathrm{C}_2 \cdot}}{\mathrm{C}_1}$ and $\mathrm{C}_2 \cdot \mathrm{C}_4$ as constants a and b, respectively, the form of the function to be used in curve-fitting is:

$$\rho = 1 - a \cdot e^{b\sqrt{T}} \qquad 4.8b$$

The temperature coefficient of reactivity is defined as:

$$\alpha_T = \frac{d\rho}{dT} \cong -\left[a \cdot e^{b \cdot \sqrt{T}} \cdot b \cdot T^{-0.5}\right] \cong -\frac{a \cdot b}{2 \cdot \sqrt{T}} \cdot e^{(b\sqrt{T})} \qquad 4.9$$

It should be noted that equation 4.9 is an approximation, based on the assumption that Doppler broadening is the dominating factor – the changes in the other factors, due to fuel temperature changes, are assumed to be much smaller (Lewis, 2008).

The MTC can be shown to also contain the resonance escape probability factor; hence the form of the function for MTC is similar to the form of the function used for FTC, as it may be with different constants in the function (Lewis, 2008). (See also equations 10 ad 11 in paragraph 2.3).

4.4 Validation calculations: Full-core Serpent model

A full core model for the proposed fuel design and reference fuel designs were simulated using a Monte-Carlo neutronic code to study the effects of temperature variation on reactivity. The calculations were done at BOC. The criticality calculations were performed using the SERPENT software. SERPENT is a continuous-energy multi-purpose Monte Carlo particle transport code (Lepp, 2013). The geometry and

material description for the fuel-pin is similar to that of the full core model. All the above-mentioned numerical methods of analysis for a fuel pin apply to the full core for FTC, MTC with 0 ppm boron and MTC with 1000ppm boron, that is, all the steps done from sections 4.1 to 4.3 were applied to the full core simulation. Figure 4-1 and Figure 4-2 show the side view of the fuel-pin model of the proposed thorium-uranium fuel and the reference uranium fuel respectively. Figure 4-3 shows the axial view of a fuel pin. The fuel assembly is made of fuel rods (fuel pins) and the full fuel core is made up of fuel assemblies. Figure 4-4 shows an equilibrium full core of a proposed fuel design and a reference fuel design which is made up of fuel rods shown in Figure 4-3. In order for the core to reach an equilibrium fuel cycle loading arrangement, a fresh fuel loading is simulated (by performing a burnup calculation using Serpent) to complete the first burnup cycle. When the first cycle is complete 1/3 of the fuel of the first cycle is replaced with fresh fuel to commence with the second burnup cycle. Upon the completion of the second cycle, the core is made up of 1/3 once burnt and 2/3 twice burnt fuel. To commence with the third cycle, 1/3 fuel of the second cycle is replaced with fresh fuel. A repeat of the core loading pattern done on the first, second and third cycle is done on the fourth cycle where 1/3 of the twice burnt fuel is replaced with fresh fuel. The firth cycle was determined to be the equilibrium cycle where the core is an equilibrium core model of the proposed fuel designs and the reference fuel as shown in Table 3.

Table 3: Core loading pattern

	Burnup Cycles				
	1	**2**	**3**	**4**	**5**
Core loading	1/3 Fresh fuel	1/3 Once-burnt fuel	1/3 Twice-burnt fuel	1/3 Fresh fuel	1/3 Once-burnt fuel
	1/3 Fresh fuel	1/3 Once-burnt fuel	1/3 Fresh fuel	1/3 Once-burnt fuel	1/3 Twice-burnt fuel
	1/3 Fresh fuel	1/3 Fresh fuel	1/3 Once-burnt fuel	1/3 Twice-burnt fuel	1/3 Fresh fuel

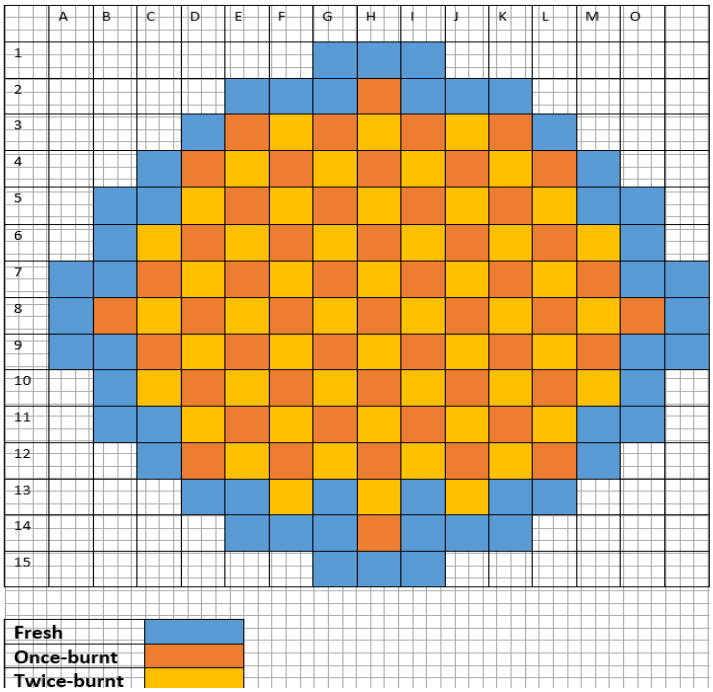

Figure 4-4: Axial view of a full-core equilibrium fuel design

5 Results and discussions

In this section the FTC and MTC for the proposed fuel designs for an equilibrium fuel pin simulation (using the MCNP transport code) as well as the whole core (based on the SERPENT code) are presented. In all instances, equilibrium fuel was used. Equilibrium fuel was obtained by replacing 1/3 of the fuel at BOC, in each cycle, until near-identical repetitive k_{eff} patterns were obtained, for all fuel models. The simulations for the proposed designs were done at three burnup positions, namely, BOC, MOC, and EOC respectively. The effective multiplication factor, MTC and FTC are represented for these burnup positions. Full-core simulations (using the SERPENT transport code) were only performed at BOC, due to the elaborate computational effort associated with full-core Monte-Carlo calculations, and because at BOC the influence of boron concentration on MTC (in conjunction with temperature variation) is the largest. In all subsequent analyses where temperature dependence on the fuel is concerned, the analysis was restricted to four temperature points (300K, 600K, 900K and 1200K) which coincide with the continuous-energy cross-section temperatures in the ENDF/B-VII data libraries.

It should always be possible to shut down a reactor in a controlled manner in all operating conditions. Transients are often associated with temperature changes which influence the fuel temperature as well as the coolant temperature. In a well-designed reactor, all the temperature coefficients of reactivity will be negative to ensure a safe regime in the case of transients. In order to see the effect of temperature change, MCNP simulations were run at a range of simulated fuel and moderator temperatures to determine the effective multiplication factor as a function of these temperature changes so as to obtain the MTC and FTC.

5.1 Fuel pin calculations at BOC, MOC and EOC models

5.1.1 Fuel temperature change

In Figure 5-1, k_{eff} as a function of fuel temperature is shown for the equilibrium fuel of the three proposed fuel designs and the reference fuel at BOC. The smooth curves fitted in the data of k_{eff} are of the form presented in Equation 4.7, as elaborated in

Paragraph 4.3.1. The k_{eff} curves of all the fuel designs have a negative slope over the entire temperature range under investigation, which indicates a negative FTC at BOC. The k_{eff} curve values are lower for fuel containing more thorium, however, the reference fuel has a slightly lower k_{eff} values than the 1Th1U fuel as shown in Figure 5-1 at temperature range below 450K. Figure 5-2 shows the multiplication factor curves as a function of fuel temperature at MOC which also has a negative gradient for all fuel models. As shown in Figure 5-2, a similar trend occurs at MOC as well as at BOC, although the k_{eff} curve values of 1Th1U at temperatures below 450K are greater than that of UO_2. In Figure 5-3, the k_{eff} against fuel temperature curves are shown at EOC, where the k_{eff} values for 3Th1U are greater than for the rest of the fuel designs and reference fuel.

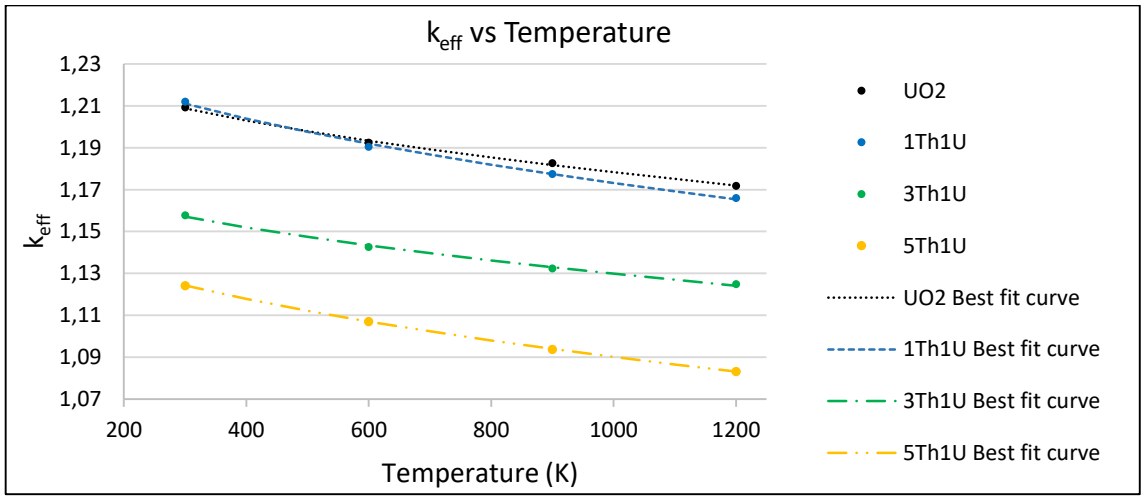

Figure 5-1: k_{eff} vs Fuel temperature at BOC

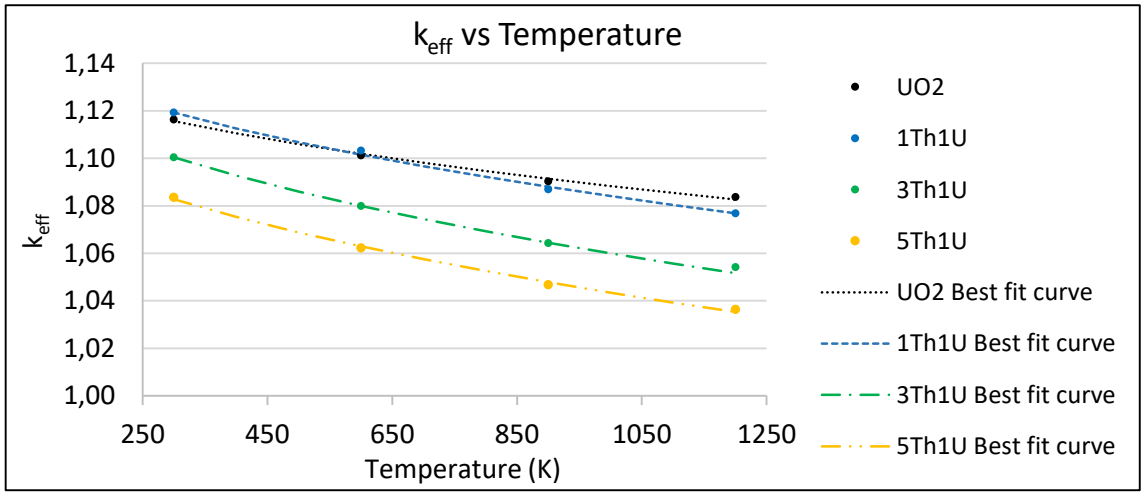

Figure 5-2: k_{eff} vs Fuel temperature at MOC

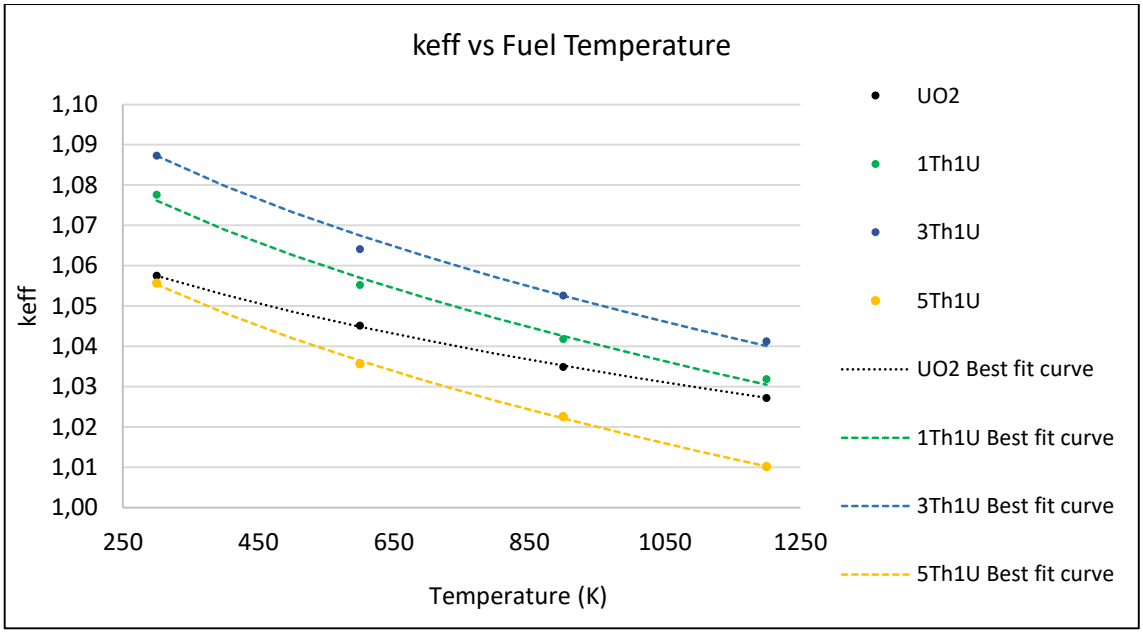

Figure 5-3: k_{eff} vs Fuel temperature at EOC

Figure 5-1, Figure 5-2 and Figure 5-3 show that as the burnup increases k_{eff} decreases, which indicates that as the fuel material matrix changes the value of k_{eff} is altered due to the material matrix changes which occur as a result of burnup and conversion. Furthermore, the k_{eff} curves in all three burnup points have a negative slope which indicates that as the temperature of the fuel at any burnup point increases the value of the effective multiplication factor decreases. This data renders results comparable to that of e.g. Uguru *et al* (2021) see also paragraph 3.2.2 that as the fuel temperature increases, k_{eff} decreases. Figure 5-1 and Figure 5-2 show that at BOC and MOC, when considering only the proposed fuel models, an increase in thorium content results in lower k_{eff} curves values, due to the absorption of neutrons by Th^{232}, prior to the phase when U^{233} is produced in significant concentration (which would produce neutrons again through fission). A general trend to observe from Figure 5-1, Figure 5-2 and Figure 5-3 is that, in all the fuel pin models the k_{eff} values decrease with burnup which is to be expected. Furthermore, the k_{eff} values also decrease with an increase in temperature in the temperature range considered.

Fuel temperature variation affects the neutron absorption in the resonance region of the nuclide cross-section due to the Doppler Effect: fuel temperature increase leads to broadening of the resonance absorption peaks, which leads to a decrease in the resonance escape probability factor (*p*). This results in a smaller k_{eff}, hence a negative

temperature coefficient of reactivity. In Figure 5-4, Figure 5-5, and Figure 5-6, FTC is shown as a function of fuel temperature within a range of 300K to 1200K fuel temperature of the three proposed fuel designs and reference model, all for equilibrium fuel. The smooth curves fitted in the data are of the equation form of Equation 4.9. The results presented in the figures show that the fuel temperature coefficients of reactivity at BOC, MOC and EOC are negative due to the Doppler broadening in the resonance region. That is, as the temperature of the proposed fuel and reference fuel changes, the resonance absorption also changes. The increasing fuel temperature results in resonance absorption increase, which decreases k_{eff}. The study done by Uguru *et al (*2020) considered six thorium-uranium mixed oxide fresh cores with different core fuel compositions to study the FTC of each core in the 500K and 2500K temperature range. The study shows that between BOC and MOC the FTC is at first negative (at BOC) and gradually increases to become positive at EOC. However, in this study at all burnup points, the FTC is negative because the proposed fuel designs and reference fuel are equilibrium fuel, which is made up of 1/3 fresh fuel, 1/3 once-burnt fuel and 1/3 twice-burnt fuel.

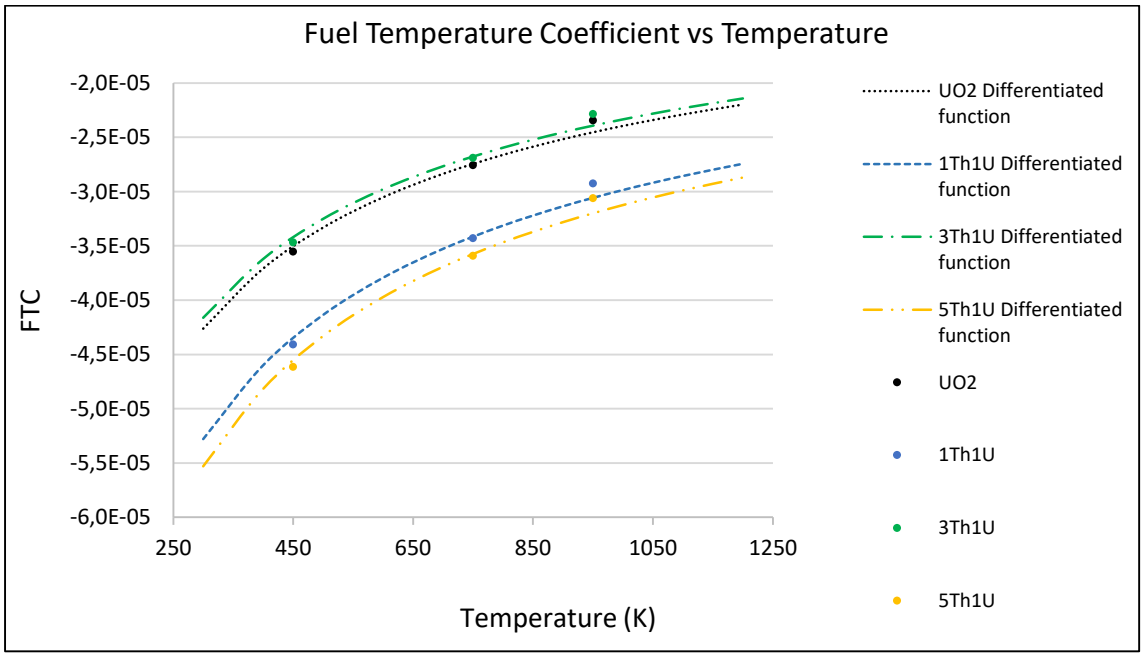

Figure 5-4: FTC vs Fuel temperature at BOC

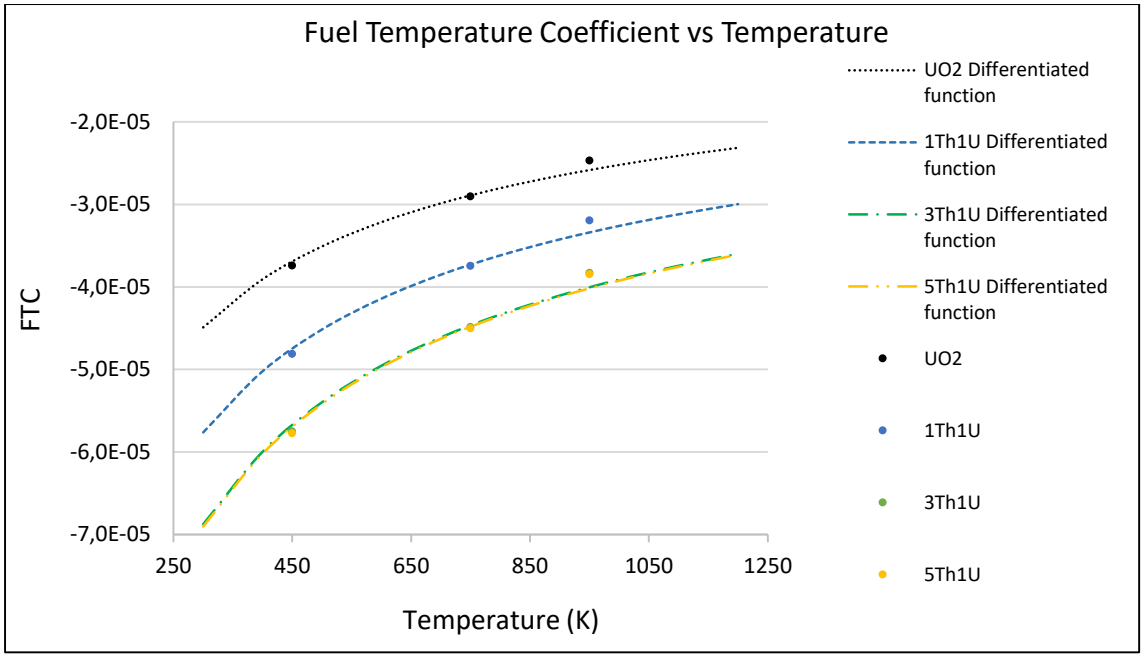

Figure 5-5: FTC vs Fuel temperature at MOC

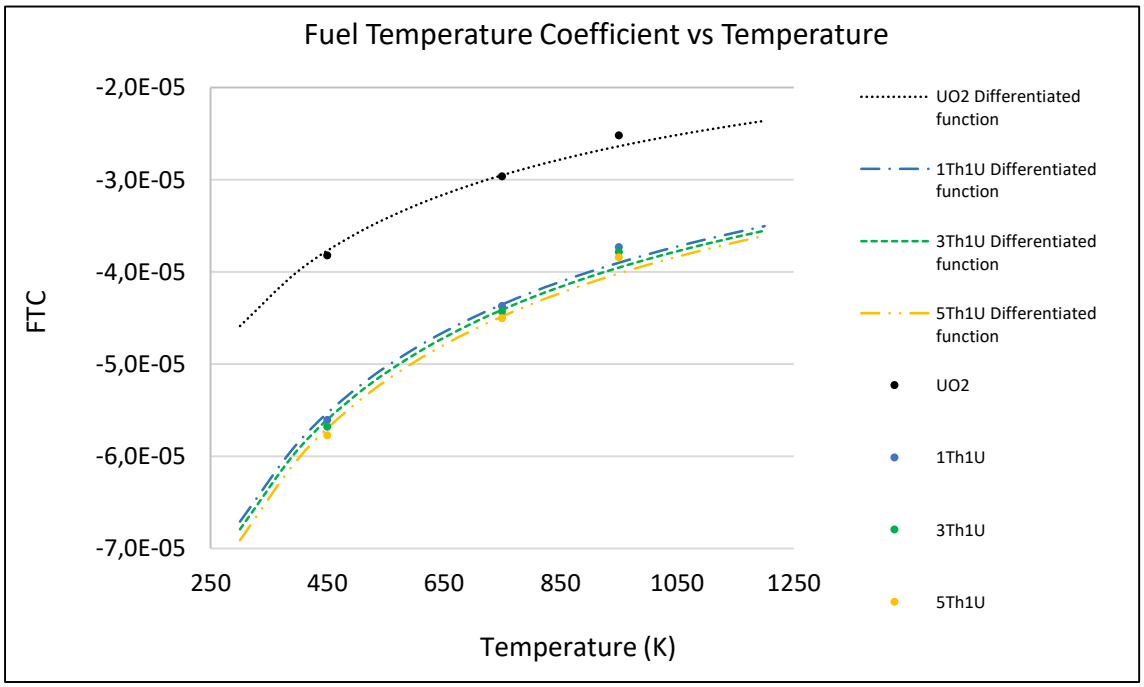

Figure 5-6: FTC vs Fuel temperature at EOC

5.1.2 Moderator temperature change.

The MTC is dominated by density changes in the moderator, which is directly influenced by a change in moderator temperature. In Figure 5-7, Figure 5-8 and Figure 5-9, k_{eff} against moderator temperature of an equilibrium fuel of three proposed fuel

designs and reference fuel are presented for all burnup points. The k_{eff} curve slopes for all burnup points are negative for all fuel models. At BOC and MOC, as shown in Figure 5-7 and Figure 5-8 respectively, the k_{eff} of the reference fuel is greater than the k_{eff} of the proposed fuel designs across the temperature range.

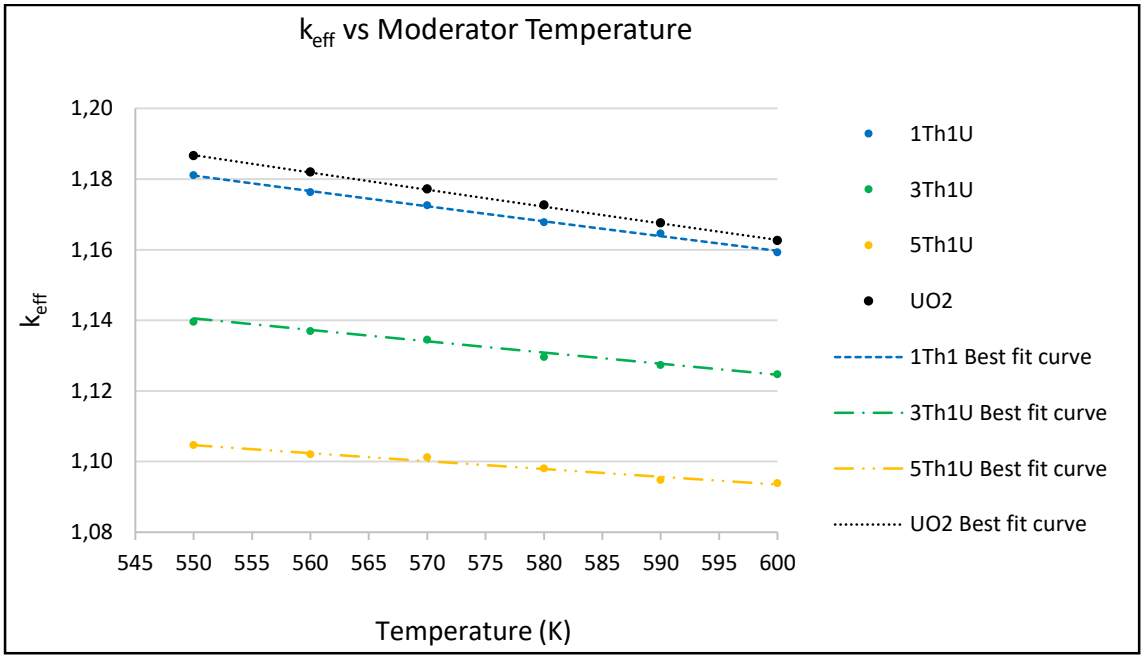

Figure 5-7: k_{eff} vs Moderator temperature without boron at BOC

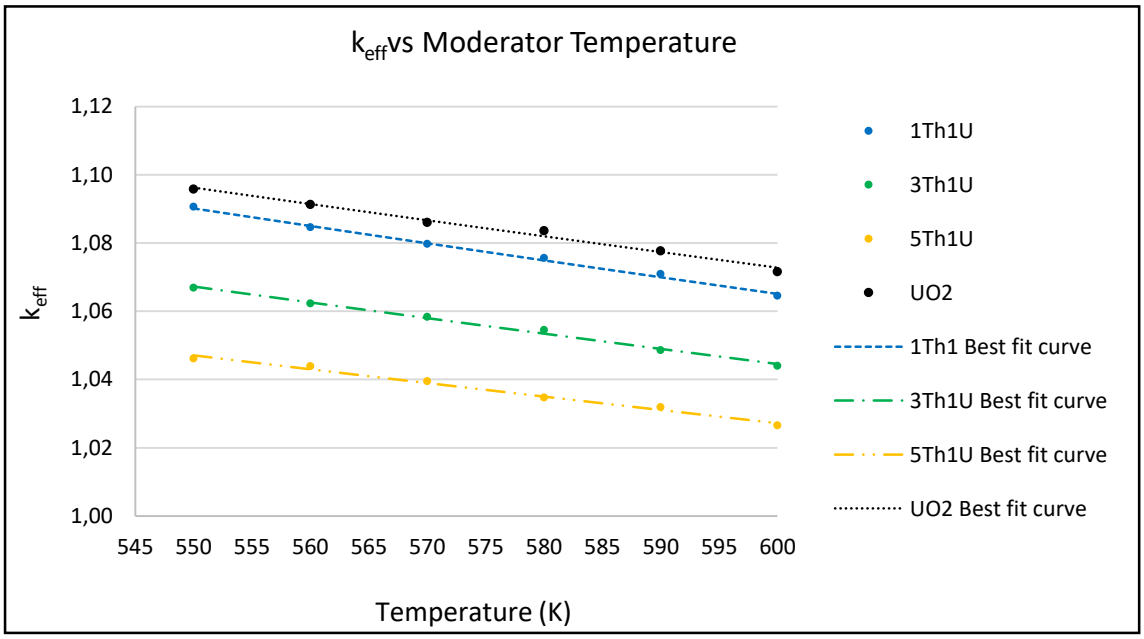

Figure 5-8: k_{eff} vs Moderator temperature without boron at MOC

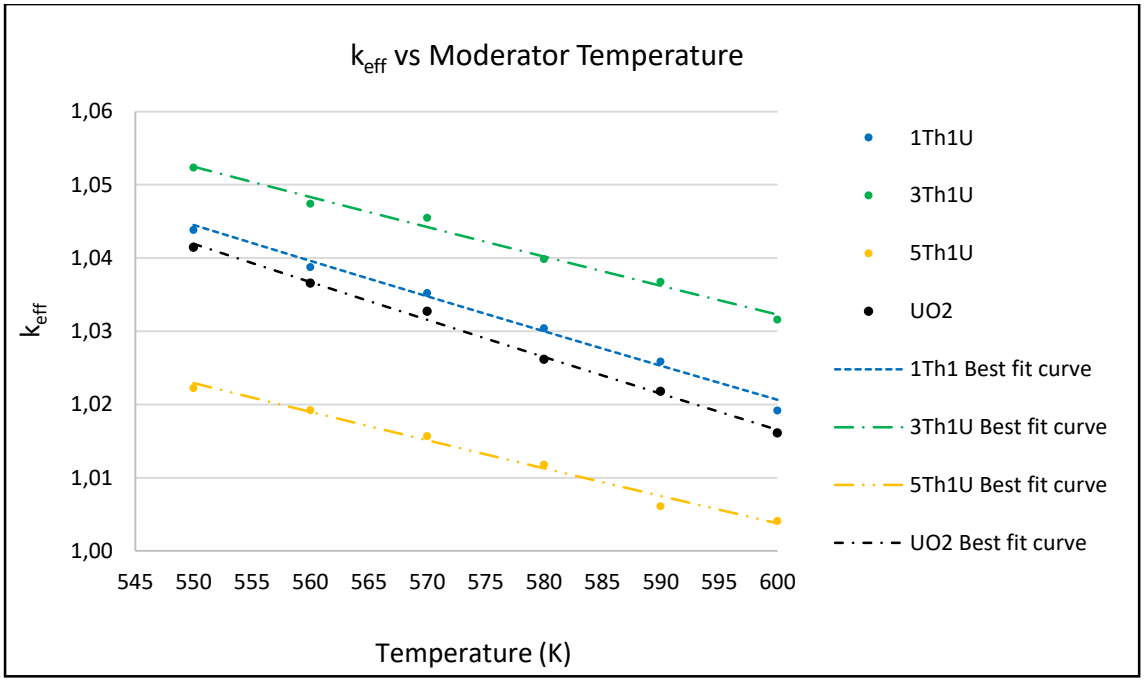

Figure 5-9: k_{eff} vs Moderator temperature without boron at EOC

With an increase in temperature of the moderator, the effective multiplication factor for all the fuel designs decreases at all the burnup points, render negative slopes on all k_{eff} curves (which indicates a negative MTC). Due to a decrease in the coolant density, thermal expansion of coolant atoms occurs which results in reduced neutron moderation, thus reducing the number of thermal neutrons, leading to reduced fissioning, which renders a decrease in k_{eff} , in other words the most probable energy of the neutron spectrum increases with temperature as shown in Figure 5-7, Figure 5-8 and Figure 5-9.

A negative slope of the k_{eff} curve as a function of temperature indicates a negative temperature coefficient of reactivity. Figure 5-10, Figure 5-11 and Figure 5-12 shows the MTC of the fuel at BOC, MOC and EOC respectively. At all the burnup points the temperature coefficient of reactivity is negative for all specified temperature ranges. At BOC, all fuel models have negative reactivity temperature coefficients, with the reference fuel being the lowest, followed by the temperature coefficients of fuel models 1Th1U, 3Th1U and 5Th1U, in that order. As the fuel cycle approaches the end of the cycle, the MTC of the reference fuel becomes more negative than the rest of the proposed fuel designs. The data shows that, as the temperature of the coolant increases, the reactivity decreases, due to the expansion of moderator that lead to a

reduction in moderation of neutrons - hence decreasing the number of thermal neutrons which are required for fission.

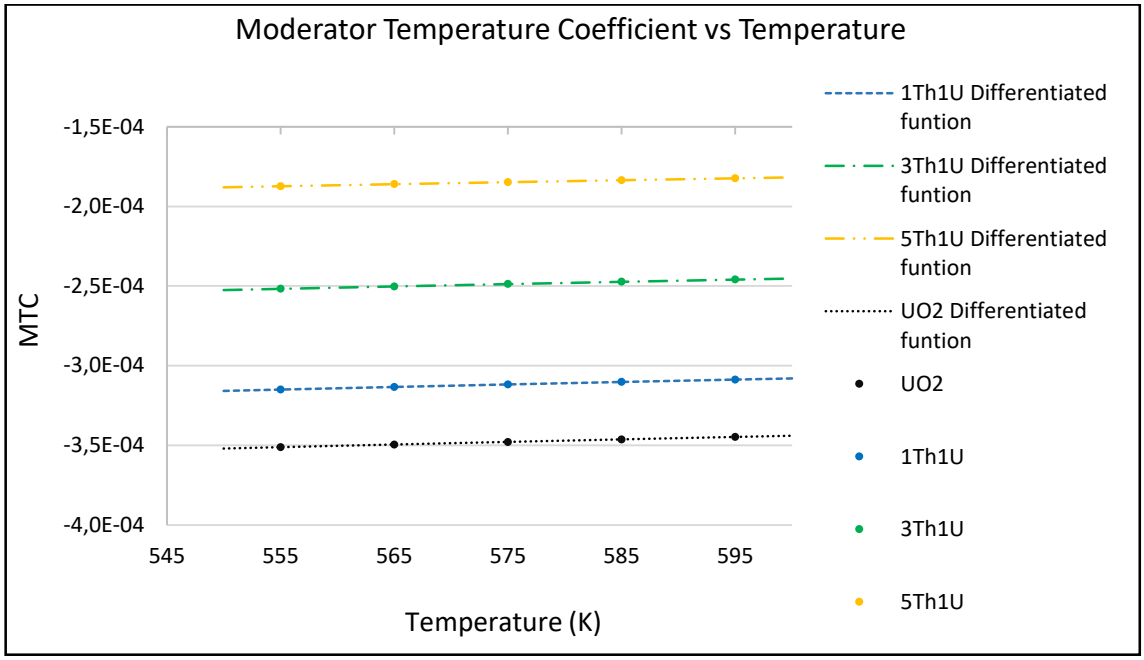

Figure 5-10: MTC vs Moderator temperature without boron at BOC

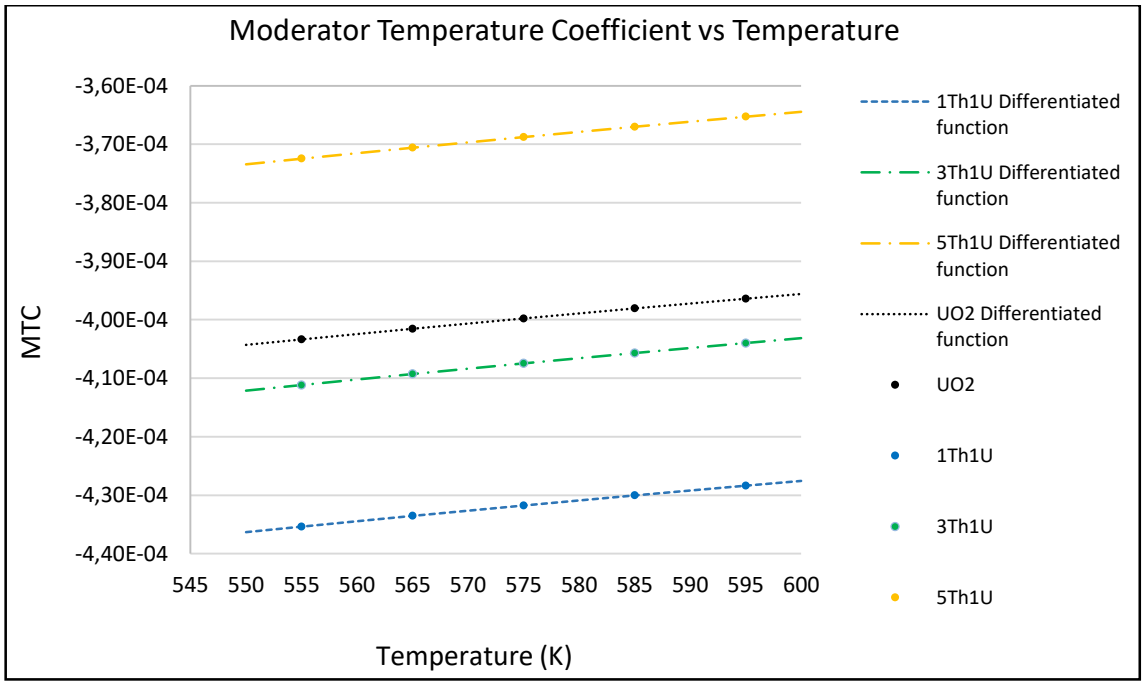

Figure 5-11: MTC vs Moderator temperature without boron at MOC

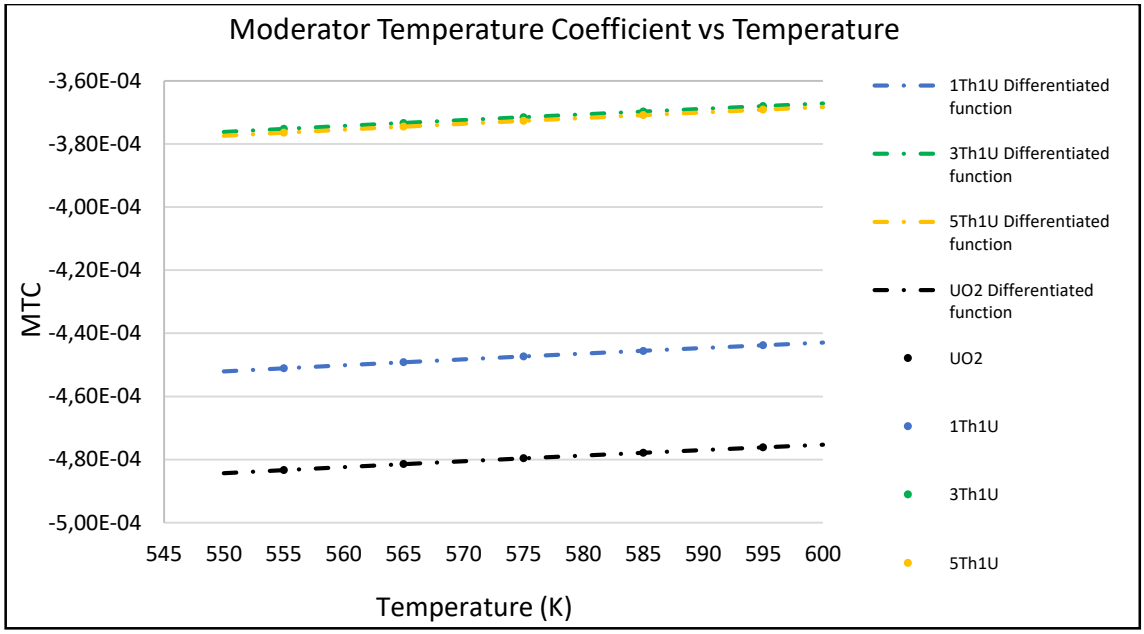

Figure 5-12: MTC vs Moderator temperature without boron at EOC

5.1.3 Moderator temperature change with 1000ppm Boron concentration.

At BOC, excess reactivity is required to allow for sufficient operation during burnup. Safe shutdown criteria limits allowable excess reactivity, at BOC. If excess reactivity is controlled by means of introducing neutron absorbers in a form of burnable poisons, reactor control is possible without distorting the flux profile of the reactor, which is inevitable if control is done by means of control rods. Boric acid is a water-soluble substance introduced into the moderator to control excess reactivity.

Figure 5-13, Figure 5-14 and Figure 5-15 show the k_{eff} against moderator temperature at BOC, MOC and EOC respectively. The 1000 ppm boric acid concentration was chosen to set up and test the models. At BOC, as illustrated in Figure 5-16, fuel designs 1Th1U, 3Th1U and the reference fuel render a supercritical reactor due to a k_{eff} above one, while the k_{eff} of 5Th1U is less than one, which indicates a subcritical reactor at these high boron concentrations. At MOC, all the proposed designs and the reference fuel are subcritical. The k_{eff} curves for 1Th1U, 3Th1U and UO_2 have a negative gradient at MOC and EOC.

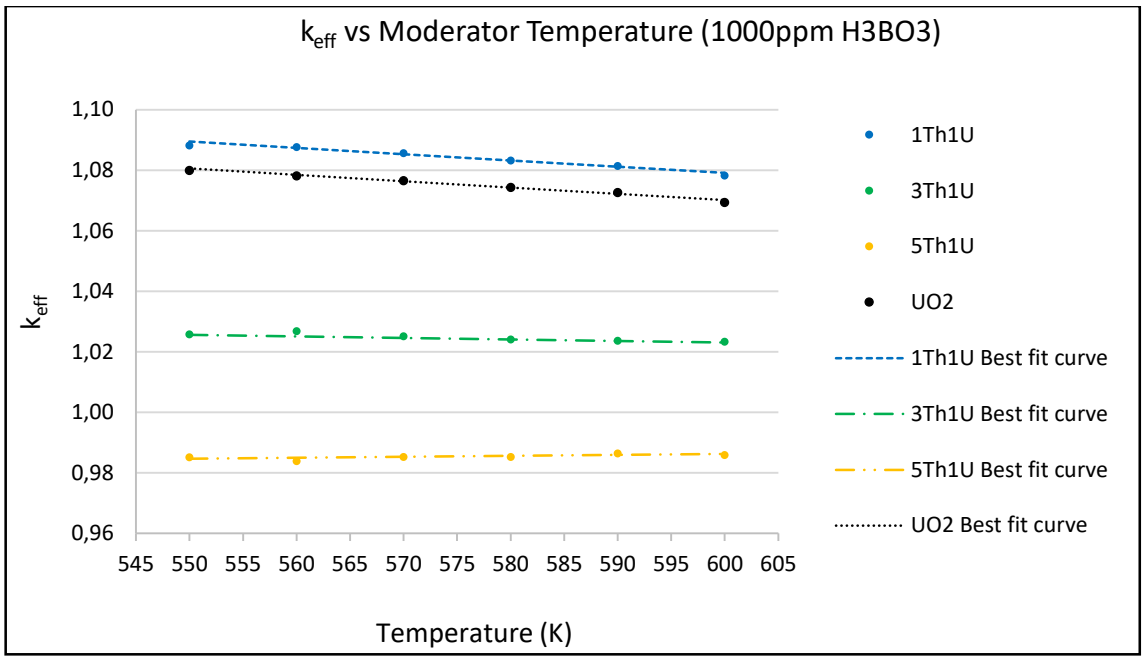

Figure 5-13: k_{eff} vs Moderator temperature with 1000ppm boron at BOC

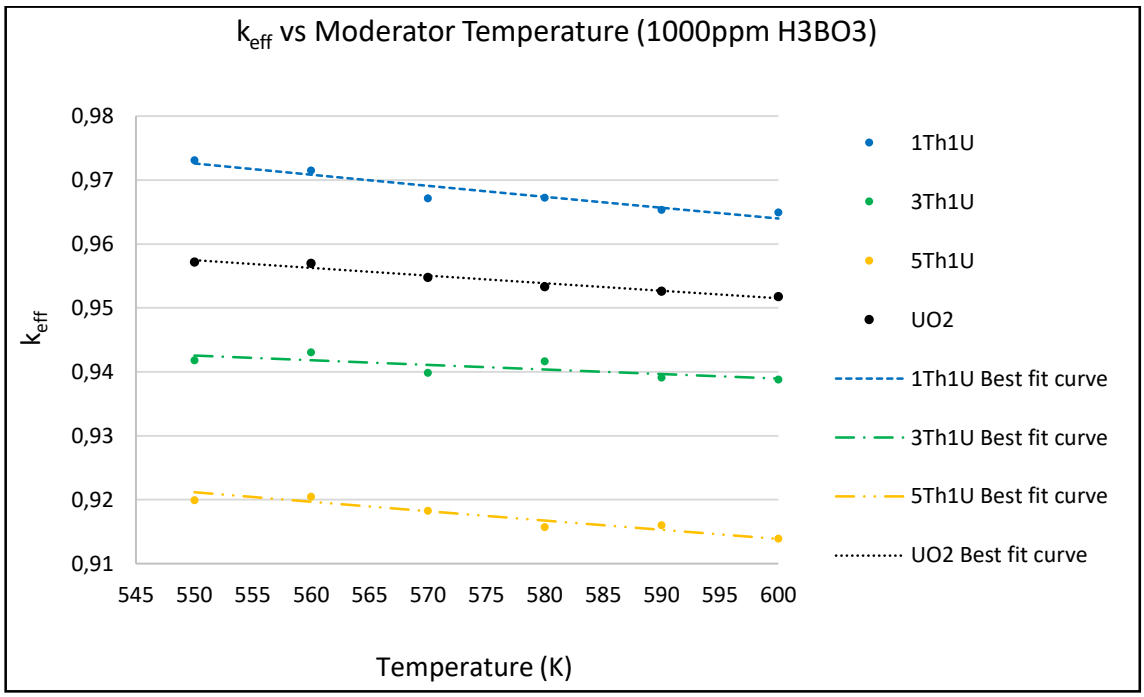

Figure 5-14: k_{eff} vs Moderator temperature with 1000ppm boron at MOC

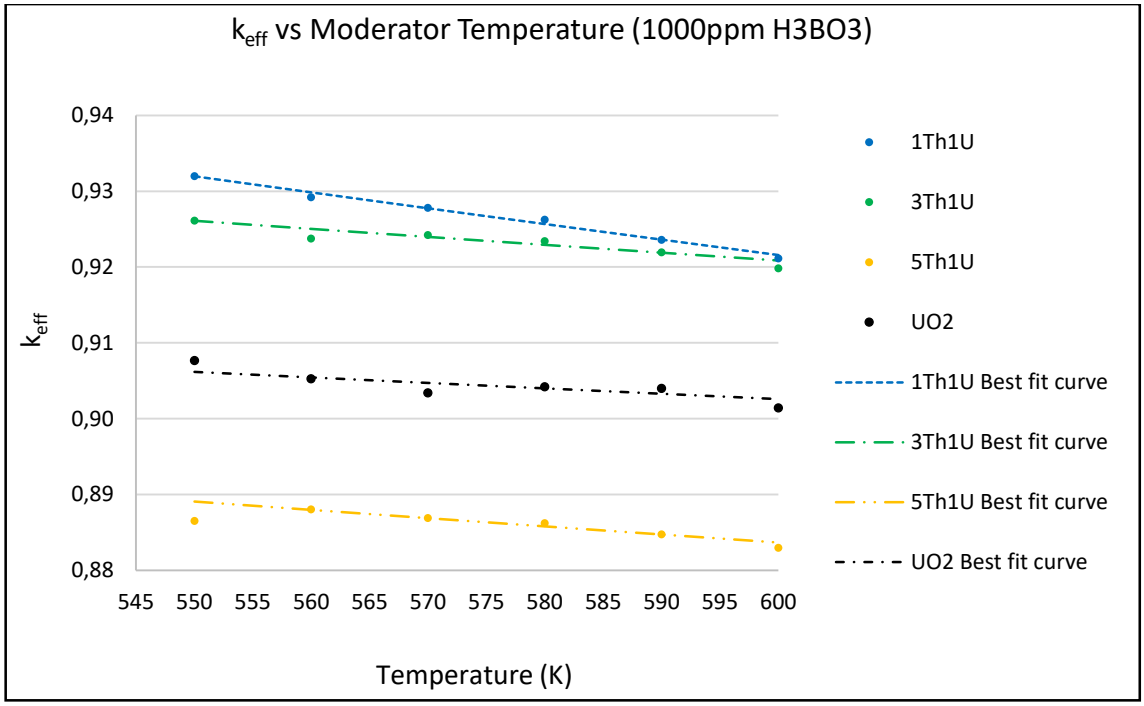

Figure 5-15: k_{eff} vs Moderator temperature with 1000ppm boron at EOC

While 1000 ppm boron specified at BOC to test the modelling setup, it is expected that boron concentration will significantly decrease towards MOC and EOC. Nevertheless, these values are presented here to test the modelling setup and to represent a scenario at the specified maximum boron concentrations levels. Figure 5-16 indicates fuel models, except for 5Th1U, have negative MTCs. Introducing boron in the 5Th1U fuel moderator at BOC rendered a positive MTC due to the coolant expansion, that is, the increased temperature decreases the coolant density which subsequently reduces the boron concentration - hence a positive reactivity this leads to heat generation which reduces the moderator density affecting the moderator effect and fuel cooling. Figure 5-17 and Figure 5-18 show that the MTC of 5Th1U improves as the burnup increases which might be attributed to the change in the fuel material composition. The study that was done by Raj and Kannan (2022)assesses the use of different fuel cycles on thorium in current LWRs. Raj and Kannan (2022) studies the importance of using thorium oxide fuel without changing the geometry of the reactor structure and comparing it to LWRs. The MTCs were calculated at 0 ppm and 600 ppm boron concentrations for a three-batch fuel assembly of the following fuel assemblies, i.e U^{235}-U^{238}, U^{235}-Th^{232} and U^{233}-Th^{232}. Raj and Kannan (2022) found that U^{235}-U^{238} and U^{235}-Th^{232} have negative MTCs at burnup points under investigation. At 0 ppm boron

concentration U^{233}-Th^{232} has a negative MTC, however, when the boron concentration is at 600 ppm, the MTC becomes positive. Therefore Raj and Kannan (2022) show that fuel containing thorium have less negative MTC compared to uranium based fuel.

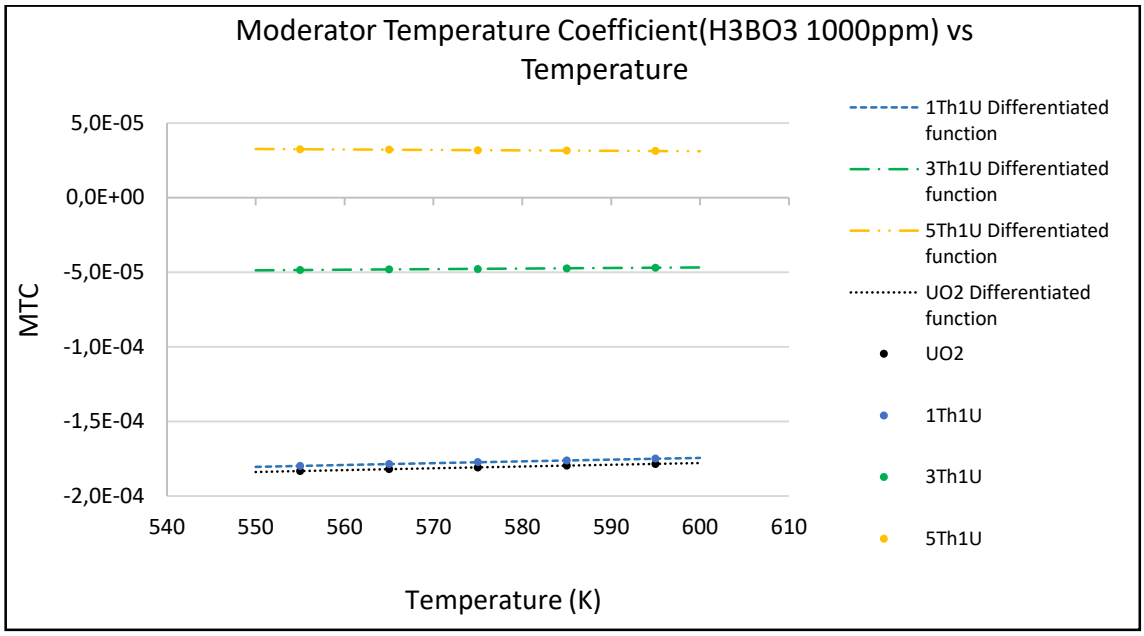

Figure 5-16: MTC vs Moderator temperature with 1000ppm boron at BOC

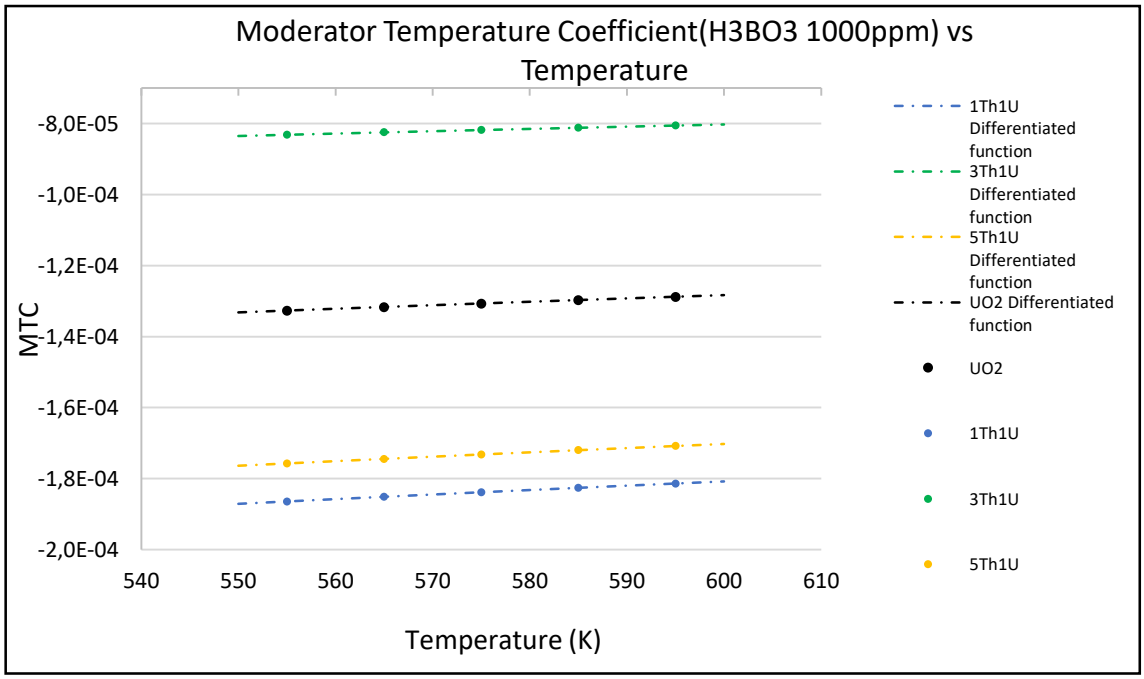

Figure 5-17: MTC vs Moderator temperature with 1000ppm boron at MOC

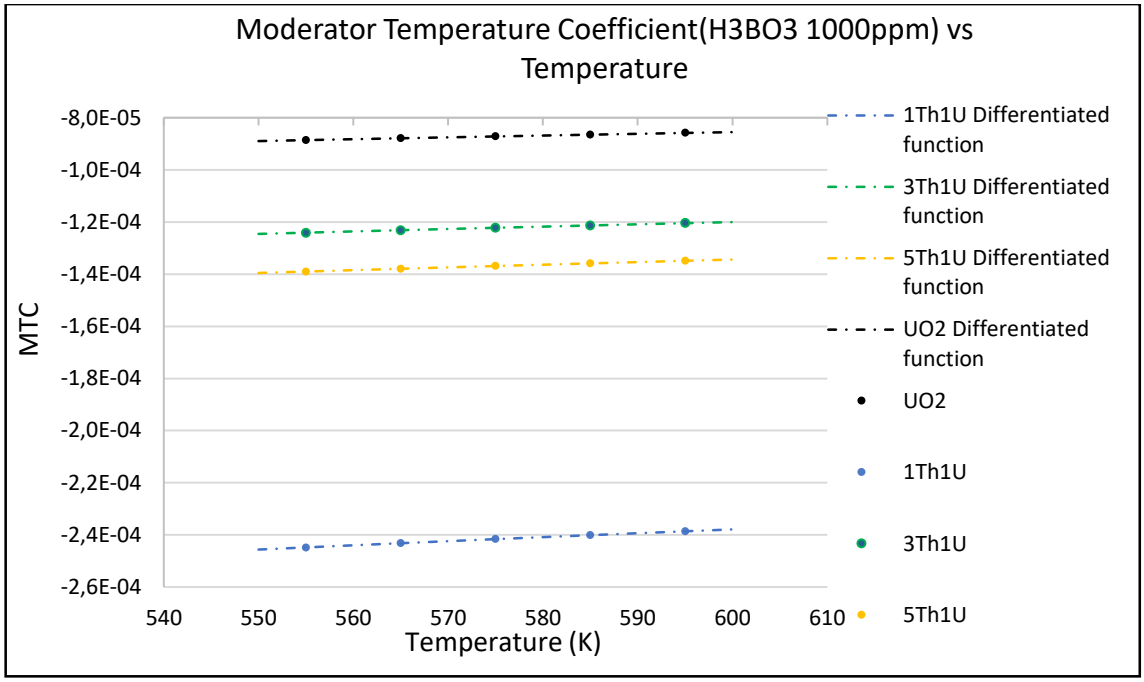

Figure 5-18: MTC vs Moderator temperature with 1000ppm boron at EOC

5.1.4 Moderator temperature change with varying boron concentration

Excess reactivity at BOC is typically compensated by using soluble neutron absorbers (boron) in the coolant and burnable poisons in the fuel. Here only the addition of soluble neutron absorbers is considered. Since thorium in fuel acts as a neutron absorber, k_{eff} at BOC is usually lower for fuel models containing more thorium than for models containing less thorium. Hence, in order to compare the fuel models in the presence of boron, the concentration of boron in the moderator for each fuel model was changed in an iterative simulation procedure until an operable reactor with k_{eff} values between 1.048 and 1.052 was obtained for each fuel model at BOC. This procedure rendered the boron concentrations used in the final k_{eff} simulations, as indicated in Table 4.

Table 4: H3BO3 concentration and k_{eff} of the fuel models at 550K moderator temperature

Fuel model	k_{eff} at 550K	H3BO3 concentration (ppm)
UO2	1.04901	1350
1Th1U	1.05048	1500
1Th1U	1.02576	750
5Th1U	0.98514	400

Figure 5-19 shows the multiplication factor as a function of the moderator temperature of the proposed fuel designs and the reference fuel. As shown in Table 4, in order to achieve k_{eff} values between 1.048 and 1.052, different boron concentrations were added to each fuel model at BOC. The table indicates that the fuel with the lowest thorium content requires the highest boron concentration for excess reactivity control for the proposed fuel designs due to thorium (Th^{232}) being a fertile isotope with a relatively high absorption cross section for neutrons.

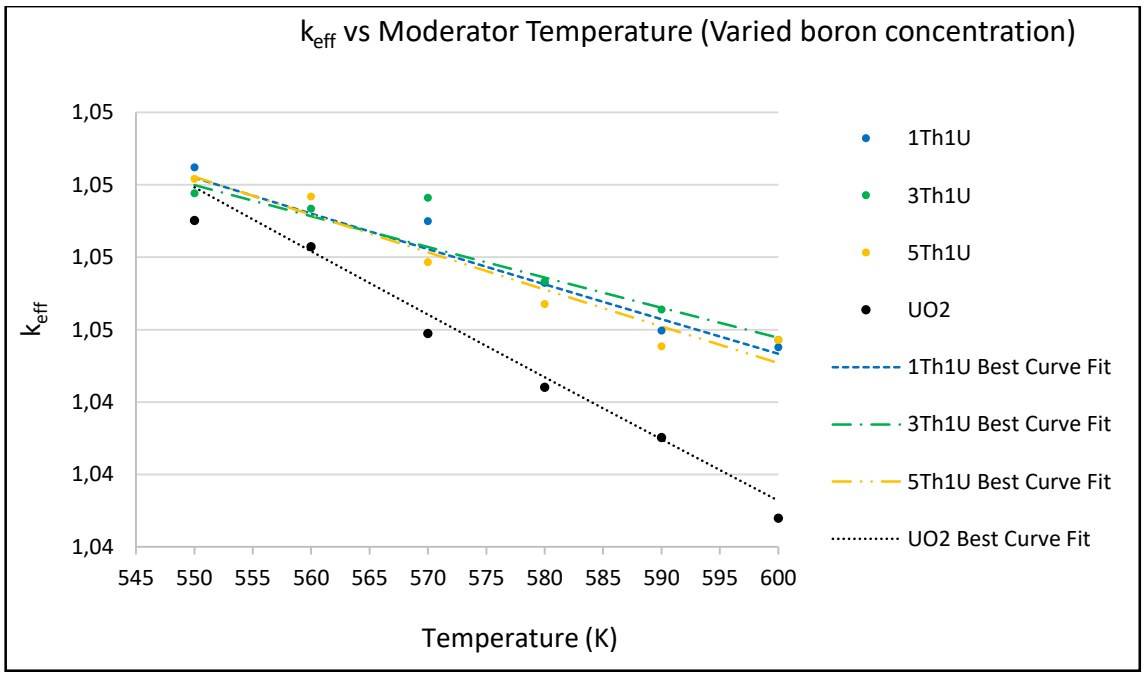

Figure 5-19: k_{eff} vs Moderator temperature (varied boron concentration) at BOC

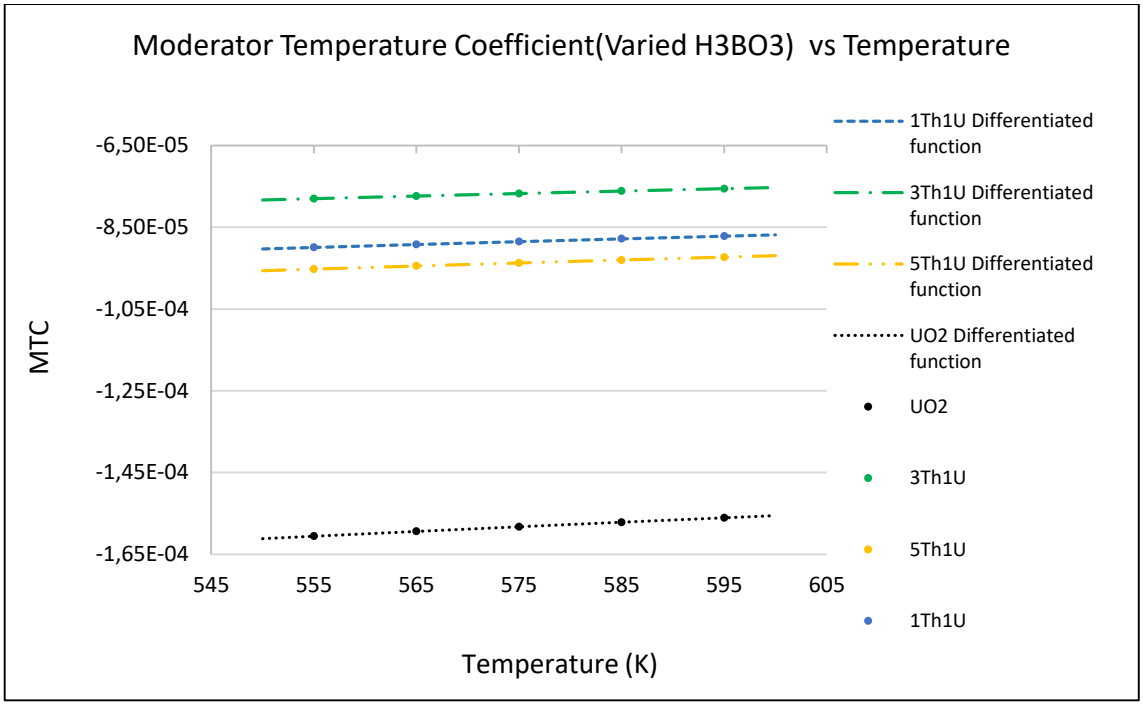

Figure 5-20: MTC vs Moderator temperature (varied boron concentration) BOC

5.1.5 Boron coefficient.

Table 5 shows the boron coefficients of an equilibrium fuel for the proposed fuel designs and the reference fuel at 550K moderator temperature BOC. The calculated boron coefficient as a function of the change in the multiplication factor and change in boron concentration is negative for all the fuel models presented in Table 5. The study done by de Stefani *et al* (2021) evaluates the use of thorium-uranium fuel by converting the Westinghouse AP1000 reactor which is fuel with UO_2, some of the parameters calculated was the boron coefficient at different burnup conditions. The boron coefficients that de Stefani *et al.* (2021) calculated for the AP1000 with UO_2 fuel and AP1000 with Th-U fuel are both negative.

Table 5: Boron coefficients for 550K moderator temperature at BOC

Fuel: UO_2		
Boron concentration (ppm)	k_{eff}	Boron Coefficient (pcm/ppm)
0	1,18666	
1000	1,07986	-10,7
1350	1,04901	-8,8
Average	1,105176667	-9,7
St Dv	0,058977854	0,9
Fuel:1Th1U		
Boron concentration (ppm)	k_{eff}	Boron Coefficient (pcm/ppm)
0	1,18113	
1000	1,0881	-9,3
1550	1,05048	-10,7
Average	1,10657	-10
St Dv	0,054913334	0,7
Fuel:3Th1U		
Boron concentration (ppm)	k_{eff}	Boron Coefficient (pcm/ppm)
0	1,13955	
1000	1,04976	-9
750	1,02576	-6,9
Average	1,07169	-7,9
St Dv	0,048974379	1,1
5Th1U		
Boron concentration (ppm)	k_{eff}	Boron Coefficient (pcm/ppm)
0	1,10462	
1000	1,05016	-5,4
400	0,98514	-18,6
Average	1,04664	-12,0
St Dv	0,048840969	6,6

5.1.6 Delayed neutron fraction

Delayed neutrons play a pivotal role in reactor controllability, particularly in events of rapid power reactor changes. Even though the number of delayed neutrons in comparison to the total number of neutrons is small, in the calculation of the effective-delayed neutron fraction they play an important role because they lengthen the effective neutron life-time since they are created by the decay of fission products that

decay with specific decay constants after the fission event that created them. Different nuclides have different fission products, each with its own decay chain. Different material matrices in fuel (changing over burnup) result in a fission fragment distribution which changes over time, hence the delayed neutron fraction changes during burnup. This accounts for the change in delayed neutron fraction obtained from the burnup simulations of different fuel models. Table 6 shows the delayed neutron fraction of the proposed fuel designs and the reference fuel at BOC, MOC and EOC. In this study average Delayed-neutron fraction of 1Th1U is larger than of UO_2. The 5Th1U and 3Th1U fuel both have a smaller β_{eff}. The study done by Galahom (2017) investigates the neutronic characteristics of four thorium-based fuel and compare them to UO_2 fuel, in the results presented the β_{eff} of Th-U^{235} is greater than that of UO_2, both fuel types contain the same amount of U^{235} enrichment, furthermore β_{eff} of both Th-U^{235} and UO_2 is larger than other suggested fuel in the study. The results presented in Table 6 in comparison to Galahom (2017) indicate that thorium-based fuel can have a larger β_{eff} depending on the fuel matrix and changes in the fuel as burnup increases. The delayed neutron fraction in all fuel models and all burnup points are considered acceptable from a reactor controllability and safety point of view when compared to the results obtain by the study of de Stefani *et al* (2021).

Table 6: Delayed neutron fractions at BOC, MOC and EOC.

	Delayed neutron fraction at three burnup points				
Fuel design	**BOC(pcm)**	**MOC(pcm)**	**EOC(pcm)**	**Average(pcm)**	**St Dv(pcm)**
1Th1U	615	465	409	496	87
3Th1U	457	400	444	434	24
5Th1U	428	593	317	446	114
UO_2	507	515	434	485	36

5.2 Equilibrium fuel full core calculations at BOC

5.2.1 Fuel temperature change

Figure 5-21 shows the k_{eff} curves against fuel temperature of proposed fuel designs and the reference fuel at BOC. The data presented show that the k_{eff} curves of the proposed fuel designs and reference fuel have a negative slope, therefore as the temperature of the fuel increases, the k_{eff} value decreases.

Figure 5-22 shows the FTC curves as a function of the fuel temperature of the proposed fuel designs and reference fuel. The FTC of the proposed fuel models and reference fuel are negative. This indicates that a full core thorium-based fuel and uranium-based fuel models have a negative feedback mechanism to fuel temperature variation.

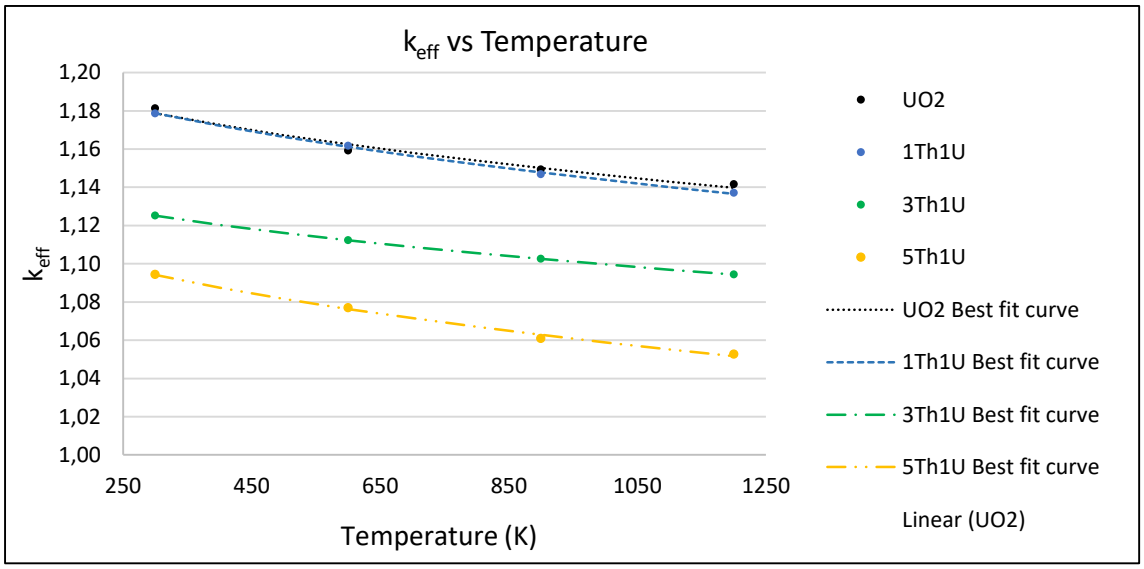

Figure 5-21: k_{eff} vs Fuel temperature of a full core at BOC

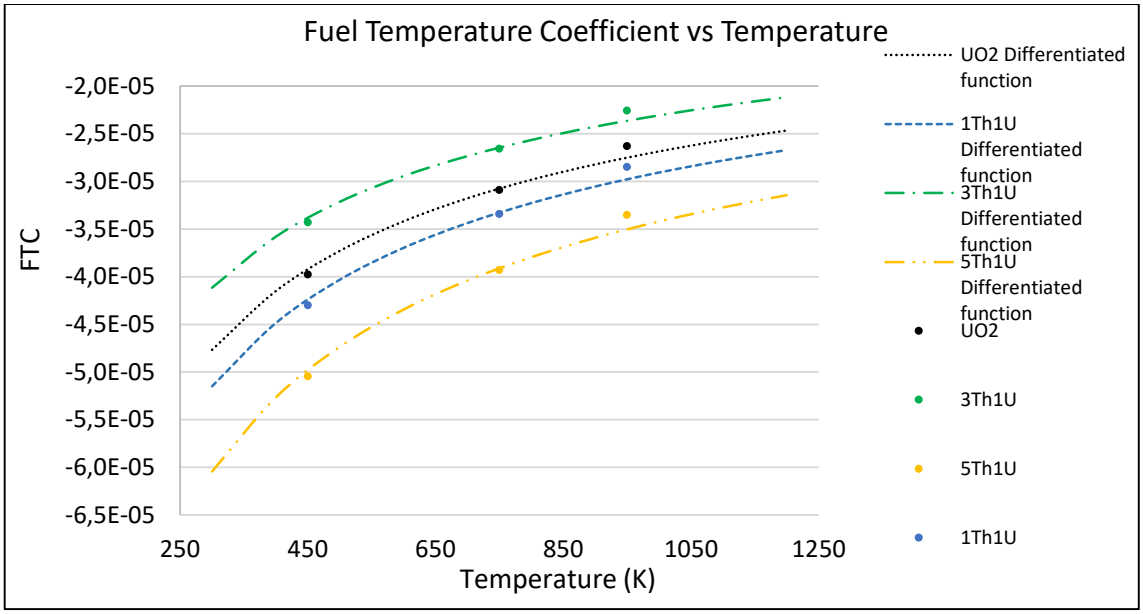

Figure 5-22: FTC vs Fuel temperature of a full core at BOC

5.2.2 Moderator temperature change without boron

The k_{eff} curves against moderator temperature of the proposed fuel designs and reference fuel is presented as shown in Figure 5-23 in the absence of boric acid. All the curves have a negative slope which indicates a negative MTC for all the fuel models presented in Figure 5-23 .The Figure 5-24shows the MTC curves against the moderator temperature of the proposed fuel designs and reference fuel. The MTC curves for all the fuel models are negative. This indicates that for a full core equilibrium fuel, increasing the moderator temperature, which will result in a reduction in moderator density, will subsequently result in a decrease in moderation, which will decrease fissions. Therefore, all full core equilibrium the MTC of all fuel models under consideration are negative, which is an important inherent safety property of the proposed fuel designs and reference fuel.

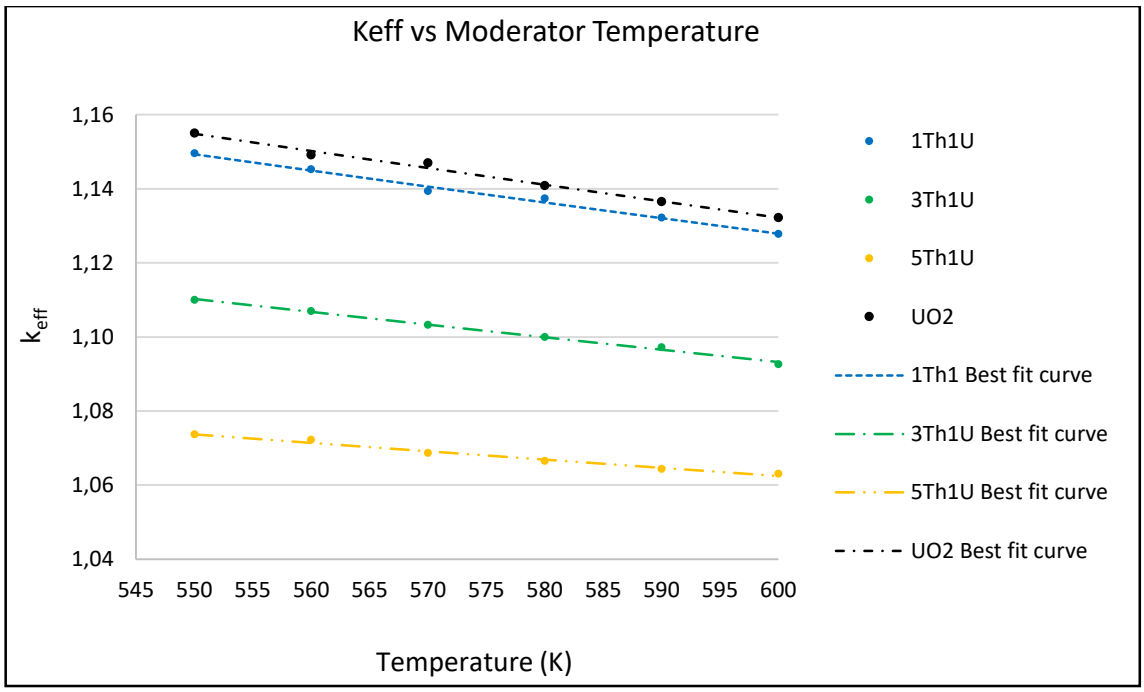

Figure 5-23: k_{eff} vs Moderator temperature of a full core without boron at BOC

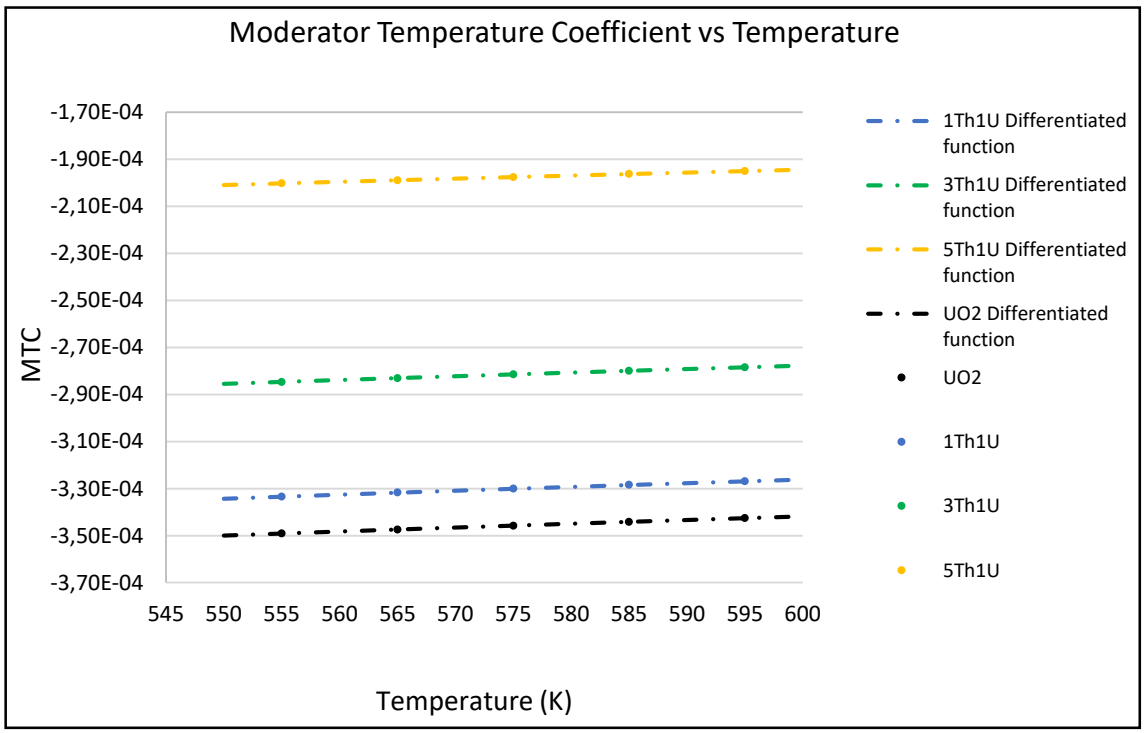

Figure 5-24: MTC vs Moderator temperature of a full core without boron at BOC

5.2.3 Moderator temperature change with 1000ppm boron.

Figure 5-25 and Figure 5-26 show the k_{eff} curves as a function of moderator temperature and MTC curves against moderator temperature of three proposed fuel designs and the reference fuel with 1000ppm boron added in the moderator, respectively. Figure 5-25 shows that adding boron to the moderator will reduce the k_{eff} and furthermore 3Th1U and 5Th1U have a k_{eff} below the critical state, therefore adding 1000ppm of boron will result in a sub-critical reactor when fuelled with 3Th1U and 5Th1U. In Figure 5-26 UO_2, 1Th1U and 3Th1U have negative MTCs, also stemming from the negative slopes of the k_{eff} curves and 5Th1U has a positive MTC due a positive slope of the k_{eff} curve.

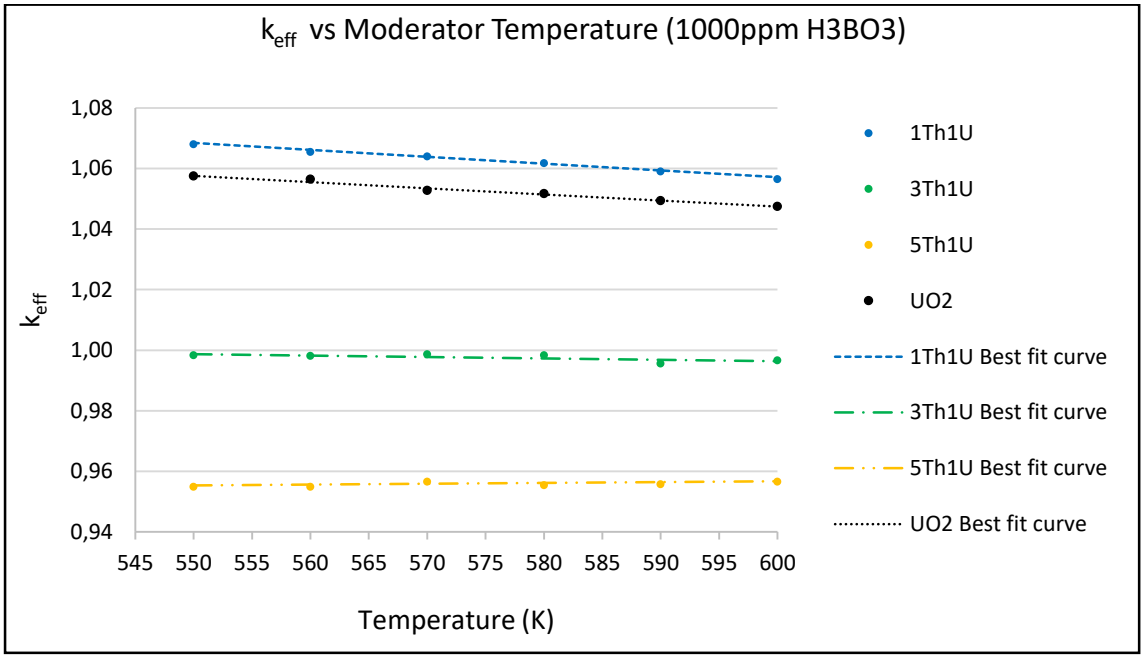

Figure 5-25: k_{eff} vs Moderator temperature of a full core with boron at BOC

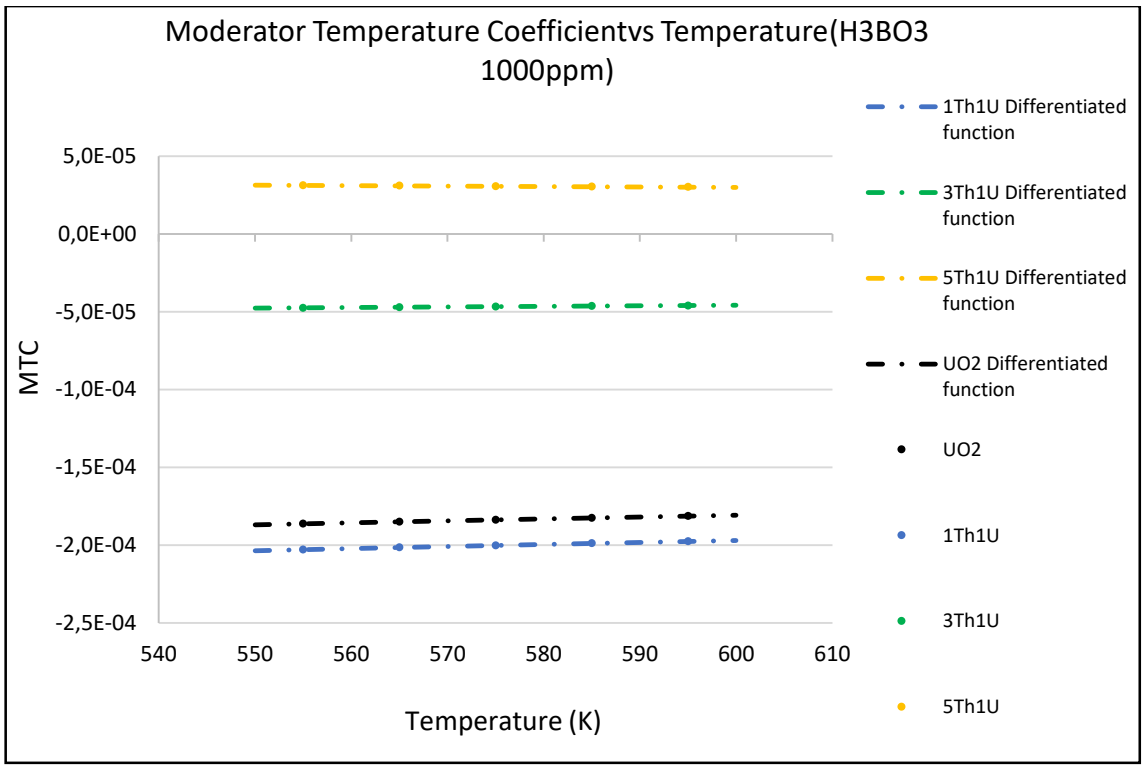

Figure 5-26: MTC vs Moderator temperature of a full core with boron at BOC

5.3 Uncertainty in k_{eff} values: MCNP (fuel pin) and SERPENT (full core) results.

The data presented in Table 7 shows the average k_{eff} of the four fuel temperature data points for a fuel-pin design modelled using MCNP and a full core design modelled using SERPENT for the three proposed fuel designs and the reference fuel. The k_{eff} for the fuel pin model is greater than that of the full core model and the difference between k_{eff} from MCNP and SERPENT for all the fuel designs is less than 3%. The k_{eff}, FTC, and MTC curves of both the fuel pin model and full core model have the same trend in terms of how these fuel designs behave when subjected to temperature variation. Table 8 presents the k_{eff} values at MOC calculated using MCNP with the standard deviations for each temperature point for FTC and MTC.

Table 7: MCNP(fuel pin) and SERPENT(full core) average k_{eff} (fuel) value comparison at BOC

	MCNP		SERPENT		Difference	
Fuel	Average k_{eff}	St Dv(pcm)	Average k_{eff}	St Dv(pcm)	pcm	%
1Th1U	1,18643	1706	1,15600	1574	2565	2,6
3Th1U	1,13942	1232	1,10859	1149	2705	2,7
5Th1U	1,10201	1536	1,07120	1593	2795	2,8
UO_2	1,18902	1375	1,15780	1485	2626	2,6

.

Table 8: Error bounds of the MCNP code calculated k_{eff} at MOC[6]

Fuel temperature change		
1Th1U		
Temperature (K)	k_{eff}	St Dv(pcm)
300	1,11932	122
600	1,10329	104
900	1,08697	168
1200	1,07681	102

Moderator temperature change without boron		
1Th1U		
Temperature (K)	k_{eff}	St Dv(pcm)
550	1,09060	118
560	1,08458	123
570	1,07975	125
580	1,07556	111
590	1,07090	111
600	1,06456	119

Moderator temperature change with 1000ppm boron		
1Th1U		
Temperature (K)	k_{eff}	St Dv(pcm)
550	0,97311	112
560	0,97149	89
570	0,96715	130
580	0,96724	110
590	0,96533	117
600	0,96494	119

3Th1U		
Temperature (K)	k_{eff}	St Dv(pcm)
300	1,11932	142
600	1,10329	94
900	1,08697	117
1200	1,07681	111

3Th1U		
Temperature (K)	k_{eff}	St Dv(pcm)
550	1,06683	122
560	1,06225	105
570	1,05833	103
580	1,05448	110
590	1,04861	104
600	1,04401	121

3Th1U		
Temperature (K)	k_{eff}	St Dv(pcm)
550	0,94183	94
560	0,94306	109
570	0,93985	106
580	0,94165	106
590	0,93908	102
600	0,93878	149

5Th1U		
Temperature (K)	k_{eff}	St Dv(pcm)
300	1,08358	111
600	1,06229	125
900	1,04681	120
1200	1,03636	89

5Th1U		
Temperature (K)	k_{eff}	St Dv(pcm)
550	1,46140	120
560	1,04392	90
570	1,03951	93
580	1,03474	146
590	1,03186	121
600	1,02658	133

5Th1U		
Temperature (K)	k_{eff}	St Dv(pcm)
550	0,91993	125
560	0,92050	114
570	0,91825	88
580	0,91570	124
590	0,91600	108
600	0,91392	111

UO2		
Temperature (K)	k_{eff}	St Dv(pcm)
300	1,11639	65
600	1,10126	67
900	1,09028	69
1200	1,08371	66

UO2		
Temperature (K)	k_{eff}	St Dv(pcm)
550	1,09580	57
560	1,09123	61
570	1,08603	62
580	1,08358	61
590	1,07768	65
600	1,07154	68

UO2		
Temperature (K)	k_{eff}	St Dv(pcm)
550	0,95718	69
560	0,95699	67
570	0,95476	58
580	0,95334	65
590	0,95262	62
600	0,95175	65

[6] Due to the small standard deviations, the error bounds are not indicated in the graphs.

6 Conclusion and recommendations

6.1 Conclusions

The study aimed to investigate the effect of fuel and moderator temperature change on the reactivity and delayed neutron fraction of the fuel proposed by Van der Walt (2015) and reference fuel at BOC, MOC and EOC. The rationale of the proposed equilibrium fuel and equilibrium reference fuel, which is made up of fresh, once and twice burned fuel respectively, was to establish which of the fuel models adhere to safety conditions with regard to negative reactivity feedback, that is, negative FTC and MTC, and whether the delayed neutron fractions are within acceptable limits during the entire operating range. The results found in this study confirm the findings by Uguru *et al* (2021) which studied the neutronic and safety parameters of a Th-U mixed oxide fuel cycle and found that the MTC and FTC for all six different cores became less negative as the temperature of the moderator and fuel respectively decreased.

The MTC and FTC of all fuel models under consideration were determined by using MCNP 6.2 (for fuel pin models) and SERPENT (for full core models) and performing burnup calculations (with MCNP models). In order to simplify the procedure, FTC and MTC were studied independently, i.e. when MTC was calculated, fuel temperature was kept constant and when FTC was calculated, moderator temperature was kept constant. While this approach is a simplification, the underlining mechanisms leading to temperature reactivity feedback (Doppler-broadening in the fuel and density changes in the moderator) can be considered independently. The FTC was determined at four fuel temperature values (300K, 600K, 900K and 1200K) due to the fact that cross section data sets were available for these data sets. This circumvented the need for calculating cross section data sets for temperature values outside these points. MTC was determined in the temperature range 500K to 600K at 10K intervals. The function used for curve-fitting in the reactivity as a function of temperature data sets, was derived from first principles by considering the six-factor formula and a number of justifiable simplifications to render a function of the form $\rho = 1 - a \cdot e^{b\sqrt{T}}$ with a and b being constants and ρ and T denoting reactivity and temperature respectively. Differentiating this function with respect to temperature (T) renders

temperature reactivity coefficients, as a function of temperature. The delayed neutron fraction for fuel pin models under consideration were calculated at a fuel temperature of 1200K for BOC, MOC and EOC respectively. The procedure to calculate delayed neutron fraction included calculating the total multiplication factor k_{total} (where prompt and delayed neutrons are considered) and the prompt multiplication factor k_{prompt} (only prompt neutrons are considered) independently using MCNP 6.2. The formula $\beta_{eff} \cong 1 - \frac{k_{prompt}}{k_{total}}$ was used to determine the delayed neutron fractions of the fuel pin models at BOC, MOC and EOC respectively.

The results indicate that for both the fuel-pin models and full-core models of equilibrium fuel, in all the thorium-uranium fuel designs and reference fuel, the FTC is negative for the temperature ranges under consideration due to the reactivity decreasing with an increase in temperature. The findings also indicate that, the FTC of the pin models and full-core models are negative at all burnup points and furthermore, the MTC (irrespective of the boron concentration) for all pin models at BOC, MOC & EOC and full-core models at BOC are negative except for 5Th1U at BOC when the boron concentration is 1000ppm.

The average delayed neutron calculated for the proposed fuel designs and reference fuel indicate that the amount of delayed neutrons emitted is distinct for each fuel design, furthermore the delayed neutron fraction varies depending on the material matrix of each fuel as burnup increase.

The results indicate that increasing the temperature of fuel and moderator, the effective multiplication factor will decrease and a negative FTC and MTC will occur at BOC, MOC and EOC.

6.2 Recommendations

This study considered fuel pin models (at BOC, MOC and EOC) and full core models (only at BOC) to determine the FTC and MTC for equilibrium fuel for the thorium-uranium-based and uranium reference fuel models and calculate fuel-pin model delayed neutron fractions at all the burnup points. It is recommended that whenever practicable, the functional form that best represents the underlying physics be used in

curve-fitting, as exemplified in this work. This method could remove fluctuations in the data, such that smooth curves of the temperature coefficient of reactivity can be obtained. Differentiation of the function so used rendered good results. Using general functions (e.g. polynomials) for curve-fitting may introduce inaccuracies, especially when differentiation of the fitted functions (in this case to obtain the FTC and MTC) is used and the degree of freedom of the function used in curve fitting is too high (to reduce errors in the points).

It is recommended that a full core calculation for equilibrium be done to determine FTC and MTC and delayed neutron fractions for the proposed fuel designs by Van der Walt (2015) for MOC and EOC.

References

Alhassan, E. *et al.* (2010) ‘analysis of reactivity temperature coefficient for light water moderated HEU-UAl4 and LEU-UO2 lattices of MNSR’, *Journal of Applied Sciences Research*, 6(9), pp. 1431–1439.

Das, N.R. (2015) ‘Nuclear materials – fissile, fertile and dual-use structural materials involved in nuclear reactors’.

Dawahra, S., Khattab, K. and Saba, G. (2016) ‘Reactivity temperature coefficients for the HEU and LEU fuel of the MNSR reactor’, *Progress in Nuclear Energy*, 88, pp. 28–32. Available at: https://doi.org/10.1016/j.pnucene.2015.11.012.

Dukert, J.M. (1970) *Thorium and the Third Fuel by*. Oak Ridge: U.S. Atomic Energy Commission - Division of Technical Information, Oak Ridge, TN. Available at: https://www.abebooks.com/Thorium-Third-Fuel-Joseph-M-Dukert/16194628850/bd.

Galahom, A.A. (2017) ‘Minimization of the fission product waste by using thorium based fuel instead of uranium dioxide’, *Nuclear Engineering and Design*, 314, pp. 165–172. Available at: https://doi.org/10.1016/j.nucengdes.2017.01.024.

Gorton, J.P. *et al.* (2019) ‘Reactor performance and safety characteristics of ThN-UN fuel concepts in a PWR’, *Nuclear Engineering and Design*, 355(July), p. 110317. Available at: https://doi.org/10.1016/j.nucengdes.2019.110317.

Hafez, N. *et al.* (2021) ‘Study on criticality and reactivity coefficients of VVER-1200 reactor’, *Progress in Nuclear Energy*, 131. Available at: https://doi.org/10.1016/j.pnucene.2020.103594.

Herring, J.S. *et al.* (2001) ‘Low cost, proliferation resistant, uranium-thorium dioxide fuels for light water reactors’, *Nuclear Engineering and Design*, 203(1), pp. 65–85. Available at: https://doi.org/10.1016/S0029-5493(00)00297-1.

Humphrey, E., Sani, S.F.A. and Uddin, M. (2020) ‘Progress in Nuclear Energy Investigation on the e ff ect of 238 U replacement with 232 Th in small modular reactor (SMR) fuel matrix’, *Progress in Nuclear Energy*, 118(February 2019), p. 103108. Available at: https://doi.org/10.1016/j.pnucene.2019.103108.

IAEA (2021) *Nuclear Power Reactors In The World*. 2nd edn. Edited by IAEA. Vienna.

International Energy AgencyIEA (2020) ‘Projected Cost of Generating Electricity’, *ORGANISATION FOR ECONOMIC CO-OPERATION AND DEVELOPMENT* [Preprint], (January). Available at: https://ncdc.gov.ng/themes/common/docs/protocols/111_1579986179.pdf.

Lamarsh, J.R. and Baratta, A.J. (2002) *Introduction to Nuclear Engineering*, *Prentice Hallrentice Hall*. Available at: https://doi.org/10.1119/1.1933896.

Lepp, J. (2013) *Serpent – a Continuous-energy Monte Carlo Reactor Physics Burnup Calculation Code*.

Lewis, E. (2008) *Nuclear Reactor Physics*. Elsevier. Available at: https://www.elsevier.com/books/fundamentals-of-nuclear-reactor-physics/lewis/978-0-12-370631-7.

Liu, B. *et al.* (2018) ‘Minor actinide transmutation characteristics in AP1000’, *Annals of Nuclear Energy*, 115, pp. 116–125. Available at: https://doi.org/10.1016/j.anucene.2018.01.031.

Nuclear Energy Agency (2015) ‘Introduction of thorium in the nuclear fuel cycle Short- to long-term considerations’, *Nuclear Energy Agency*, 1, p. 133. Available at: https://www.oecd-nea.org/science/pubs/2015/7224-thorium.pdf.

Oka, Y. (2014) *Nuclear reactor designs [3]*. Edited by Oka Yoshiaki. Springer. Available at: http://link.springer.com/10.1007/978-4-431-54898-0.

Pinem, S. *et al.* (2018) ‘Reactivity Coefficient Calculation for AP1000 Reactor Using the NODAL3 Code’, *Journal of Physics: Conference Series*, 962(1). Available at: https://doi.org/10.1088/1742-6596/962/1/012057.

Raj, D. and Kannan, U. (2022) ‘Analysis for the use of thorium based fuel in LWRs’, *Annals of Nuclear Energy*, 174, p. 109162. Available at: https://doi.org/10.1016/j.anucene.2022.109162.

René, M. (2017) ‘Nature, Sources, Resources, and Production of Thorium’, *Descriptive Inorganic Chemistry Researches of Metal Compounds* [Preprint], (September). Available at: https://doi.org/10.5772/intechopen.68304.

Serfontein, D.E. and Mulder, E.J. (2014) ‘Thorium-based fuel cycles : Reassessment of fuel economics and proliferation risk’, *Nuclear Engineering and Design*, 271, pp. 106–113. Available at: https://doi.org/10.1016/j.nucengdes.2013.11.018.

de Stefani, G.L., Maiorino, J.R. and de Losada Moreira, J.M. (2021) 'The AP-Th 1000 – An advanced concept to use MOX of thorium in a closed fuel cycle', *International Journal of Energy Research*, 45(8), pp. 11642–11655. Available at: https://doi.org/10.1002/er.5421.

Du Toit, M.H. and Cillers, A.C. (2014) 'Preliminary economic evaluation of thorium-based fuels in PWRs', *Nuclear Technology*, 187(3), pp. 260–269. Available at: https://doi.org/10.13182/NT13-134.

du Toit, M.H. and Naicker, V.V. (2018) 'Neutronic design of homogeneous thorium / uranium fuel for 24 month fuel cycles in the European pressurized reactor using MCNP6', *Nuclear Engineering and Design*, 337(July), pp. 394–405. Available at: https://doi.org/10.1016/j.nucengdes.2018.07.023.

Tucker, L.P., Alajo, A. and Usman, S. (2015) 'Annals of Nuclear Energy Thorium-based mixed oxide fuel in a pressurized water reactor : A beginning of life feasibility analysis with MCNP', *Annals of Nuclear Energy*, 76, pp. 323–334. Available at: https://doi.org/10.1016/j.anucene.2014.09.058.

Uguru, E.H. *et al.* (2020) 'Determination of the combined effect of boron and gadolinia on the reactivity and safety parameters of (U, Th)O2fuel', in *IOP Conference Series: Materials Science and Engineering*. Institute of Physics Publishing. Available at: https://doi.org/10.1088/1757-899X/785/1/012004.

Uguru, E.H. *et al.* (2021) 'Burn-up calculation of the neutronic and safety parameters of thorium-uranium mixed oxide fuel cycle in a Westinghouse small modular reactor', *International Journal of Energy Research*, 45(8), pp. 12013–12028. Available at: https://doi.org/10.1002/er.6000.

Van der Walt, H.B. (2015) 'A Heterogeneous Thorium-based fuel design for a PWR aimed at increasing fuel cycle length', (November).

Zainuddin, N.Z., Parks, G.T. and Shwageraus, E. (2016) 'The factors affecting MTC of thorium–plutonium-fuelled PWRs', *Annals of Nuclear Energy*, 98, pp. 132–143. Available at: https://doi.org/10.1016/j.anucene.2016.07.034.

Annexures

Figure 0-1 and Figure 0-2 show the cell card and material cards, respectively, of the input file for fuel temperature at 300K

```
C Cell cards
c ===========================================================
1 1  -10.04   -1 -4 -5     vol=0.26351  tmp=2.5850e-8  imp:n=1      $Fresh Th          [1/2Tn]  @300K
2 2  -10.4215 -1 -4 5 -6   vol=0.52702  tmp=2.5850e-8  imp:n=1      $Fresh 18%U        [Tn]     @300K
3 3  -10.04   -1 -4 6 -7   vol=0.52702  tmp=2.5850e-8  imp:n=1      $Twice burned Th   [T2]     @300K
4 4  -10.4215 -1 -4 7 -8   vol=0.52702  tmp=2.5850e-8  imp:n=1      $Twice burned 18%U [T2]     @300K
5 5  -10.04   -1 -4 8 -9   vol=0.52702  tmp=2.5850e-8  imp:n=1      $Once burned Th    [T1]     @300K
6 6  -10.4215 -1 -4 9 -10  vol=0.52702  tmp=2.5850e-8  imp:n=1      $Once burned 18%U  [T1]     @300K
7 7  -10.04   -1 -4 10     vol=0.26351  tmp=2.5850e-8  imp:n=1      $Fresh Th          [1/2Tn]  @300K
8 8  -0.164  1 -2 -4   vol=0.12867      tmp=7.7553e-8  imp:n=1      $He-4 clad gap        @900K
9 9  -6.56   2 -3 -4   vol=0.96178      tmp=6.8936e-8  imp:n=1      $Zircaloy-4 cladding  @800K
10 10 -0.7137  3 -4    vol=5.27303      tmp=5.6011e-8  imp:n=1      $H2O moderator        @650K
11 0  4                                                imp:n=0      $Void cell
```

Figure 0-1: Cell card for 300K Input file

```
c ======================= Material Cards ================== [temperature that data was evaluated at]
m1   90232.80c   1
      8016.80c    2
     92234.80c 3.33333E-40      92236.80c 3.33333E-40      92237.80c 3.33333E-40
     93235.80c 3.33333E-40      93236.80c 3.33333E-40      93237.80c 3.33333E-40      93238.80c 3.33333E-40
     94236.80c 3.33333E-40      94237.80c 3.33333E-40      94238.80c 3.33333E-40      94239.80c 3.33333E-40
     91232.80c 3.33333E-40      91233.80c 3.33333E-40      90231.80c 3.33333E-40       6012.80c 3.33333E-40
     90233.80c 3.33333E-40      31069.80c 3.33333E-40      31071.80c 3.33333E-40      32070.80c 3.33333E-40
     32072.80c 3.33333E-40      32073.80c 3.33333E-40      32074.80c 3.33333E-40      32076.80c 3.33333E-40
     33074.80c 3.33333E-40      33075.80c 3.33333E-40      34074.80c 3.33333E-40      34076.80c 3.33333E-40
     34077.80c 3.33333E-40      34078.80c 3.33333E-40      34079.80c 3.33333E-40      34080.80c 3.33333E-40
     34082.80c 3.33333E-40      35079.80c 3.33333E-40      35081.80c 3.33333E-40      36078.80c 3.33333E-40
     36080.80c 3.33333E-40      36082.80c 3.33333E-40      36083.80c 3.33333E-40      36084.80c 3.33333E-40
```

Figure 0-2: Material card 300K input file

Figure 0-3 and Figure 0-4 show the cell card and material cards respectively, of the input file for moderator temperature at 550k

```
c ===========================================================
C Cell cards
c ===========================================================
1 1  -10.04   -1 -4 -5     vol=0.26351  tmp=8.6170e-8  imp:n=1      $Fresh Th          [1/2Tn]  @1000K
2 2  -10.4215 -1 -4 5 -6   vol=0.52702  tmp=1.0340e-7  imp:n=1      $Fresh 18%U        [Tn]     @1200K
3 3  -10.04   -1 -4 6 -7   vol=0.52702  tmp=8.6170e-8  imp:n=1      $Twice burned Th   [T2]     @1000K
4 4  -10.4215 -1 -4 7 -8   vol=0.52702  tmp=1.0340e-7  imp:n=1      $Twice burned 18%U [T2]     @1200K
5 5  -10.04   -1 -4 8 -9   vol=0.52702  tmp=8.6170e-8  imp:n=1      $Once burned Th    [T1]     @1000K
6 6  -10.4215 -1 -4 9 -10  vol=0.52702  tmp=1.0340e-7  imp:n=1      $Once burned 18%U  [T1]     @1200K
7 7  -10.04   -1 -4 10     vol=0.26351  tmp=8.6170e-8  imp:n=1      $Fresh Th          [1/2Tn]  @1000K
8 8  -0.164  1 -2 -4   vol=0.12867      tmp=7.7553e-8  imp:n=1      $He-4 clad gap        @900K
9 9  -6.56   2 -3 -4   vol=0.96178      tmp=6.8936e-8  imp:n=1      $Zircaloy-4 cladding  @800K
10 10 -0.7600  3 -4    vol=5.27303      tmp=4.7392e-8  imp:n=1      $H2O moderator        @550K
11 0  4                                                imp:n=0      $Void cell
```

Figure 0-3: Cell card for 550K Input file

```
1207    m10     1001.81c    +2          $ Hydrogen in Water [600K]
1208            8016.81c    +1          $ Oxygen in Water. [600K]
1209    mt10    lwtr.26t                $ Scattering data for Hydrogen in Lwtr  [650K]
```

Figure 0-4: Material card 550K input file